On the fall process of rock during Subsea Rock Installation

1-D modelling of the falling process in the fall pipe

M.A. Stoter

TUDelft
Delft
University of
Technology

Challenge the future

ON THE FALL PROCESS OF ROCK DURING SUBSEA ROCK INSTALLATION

1-D MODELLING OF THE FALLING PROCESS IN THE FALL PIPE

by

M.A. Stoter

in partial fulfillment of the requirements for the degree of

Master of Science
in Offshore and Dredging Engineering

at the Delft University of Technology,
to be defended publicly on Tuesday September 25, 2018 at 13:30.

Thesis committee:	Dr. ir. G. H. Keetels	TU Delft
	Prof. dr. ir. C. van Rhee	TU Delft
	Dr. ir. W. P. Breugem	TU Delft
	Ir. A. van Es	Van Oord

This thesis is confidential and cannot be made public until December 31, 2022.

An electronic version of this thesis is available at `http://repository.tudelft.nl/`.

Acknowledgements

This thesis is the final product of my graduation research, performed in order to complete the master degree in Offshore Engineering with a specialization in Dredging Engineering at Delft University of Technology. This research could not have been realised without the help of my supervisors. So, before talking about subsea rock installation I would like to thank the people who supported me during this research.

First of all, I would like to thank Van Oord for providing me the opportunity to work on this research. In special, I want to thank Aad van Es, Frank Renting and Daniel Liefferink for their help over the duration of the project.

I also want to thank my supervisors from the Delft University of Technology, Cees van Rhee and Geert Keetels for their advice and suggestions.

A special thanks goes to my parents for their support during my entire study and providing me the opportunities to achieve my goals. And last but not least, my girlfriend, Nousjka for supporting me whenever I needed it.

M.A. Stoter
Rotterdam, August 2018

Summary

Scarcity of (green) energy resources drives mankind further offshore and towards deeper waters. Protection of subsea infrastructure is of eminent importance in these environments. The key parameter to have a good control on the installation of rock is the falling time. For larger water depths up to 1200 meters, the accuracy of the falling time prediction becomes more important because a small deviation can result in a large difference between prediction and reality. This results in production losses and off target subsea installation work.

In the offshore industry there are two types of fallpipe vessels used. Namely a closed fallpipe and a semi-closed fallpipe. A closed fallpipe consists of multiple pipe sections connected to each other while a semi-closed fallpipe consists of multiple open-ended buckets connected by two chains. The main difference between the two systems is that for a closed fallpipe the inflow of water can be controlled by a special inlet section. For a semi-closed fallpipe, water can flow freely in or out of the fallpipe through the openings between the buckets. The water will only flow in or out of the system if there is an under or overpressure in the fallpipe compared to the hydrostatic (outer) pressure. The total fall velocity of the rock depends on the settling velocity with respect to the mixture velocity and the mixture velocity itself.

The models which are currently used to determine the falling time of rock during subsea rock installation are using the equilibrium settling velocity, the hindered settling velocity or only the mixture velocity (bulk velocity). The total fall velocity of the rock is a combination of the mixture velocity and the settling velocity. To describe the fall process of rock and to determine the falling time a new model is needed. This model should include the development of the mixture velocity, the settling velocity of the rock and the possibility of water in and outflow of the element.

This thesis focuses on modelling the fall process of rock in a fallpipe during subsea rock installation. This has been done by using the drift-flux model. In this model a mixture velocity and a slip velocity (settling velocity of rock) are calculated and used in the transport equation to describe the concentration profile in the fallpipe. To determine the mixture velocity, the fractional step method is used. By using this method the intermediate velocity and pressure are calculated separately. The mixture velocity for the new time step can be calculated by correcting the intermediate velocity for the pressure, this way the new mixture velocity satisfies continuity.

The main goal of this research is to conduct a model to predict the falling time of the rocks in a semi-closed fallpipe during subsea rock installation. To do this a literature study has been carried out to look at the processes involved during subsea rock installation. When looking at the closed fallpipe the only friction loss which is taken into account is wall friction. For a semi-closed fallpipe there are also Carnot losses which have a significant contributions to the total pressure loss. Another difference between the two fallpipe systems is that for a closed fallpipe the water inflow is only at the inlet section, while for a semi-closed fallpipe water will flow freely in or out at each segment. To model this it is chosen to implement a mass source/sink in the continuity equation and a momentum source/sink in the momentum equation. The amount of water flowing in or out depends on the flow area and the flow velocity. The flow velocity is limited based on the pressure difference between in and outside of the fallpipe. The flow velocity can be calculated by Bernoulli's equation.

When the process of rock installation starts and the first rocks are falling in the fallpipe, an overpressure will be generated resulting in an outflow of water in the fallpipe. When using a closed fallpipe the outflow will be at the end of the pipe. For a semi-closed fallpipe, the outflow will take place at the spacings between the buckets, which means an overpressure will be levelled out at the opening. When the process continues, the water level in the fallpipe will drop. This is because of the increase of mixture density in the fallpipe. When the pressure in the fallpipe is lower than outside the fallpipe, water will start flowing in and generate a mixture flow in the fallpipe.

The semi-closed fallpipe model, which is obtained during this research, shows good results compared to the measurements of Van Oord. The model is one dimensional in z-direction and takes into account the wall friction, Carnot losses, hindered settling and in and outflow of water between the buckets if there is respectively an under or over pressure in the fallpipe. By using this model a good prediction of the falling time and output production can be made for a wide range of operational conditions. In this way the model can assist to reduce production losses and improve installation accuracy.

Contents

Nomenclature

Acronyms

Symbol	Description	Unit
ROV	Remotely operated vehicle	
SRI	Subsea rock installation	

Greek Symbols

Symbol	Description	Unit
α_f	Concentration of fluid	–
α_s	Concentration of solids	–
$\alpha_{s,i}$	Concentration of solids in the i$^{\text{th}}$ element	–
$\alpha_{s,k}$	Concentration of solids for fraction k	–
β	Slope of divergence	rad
Δ	Relative density	–
Δp	Pressure difference between inner and outer side of the fallpipe	Pa
Δt	Time step	s
Δx	Spacial step in x-direction	m
Δz	Spacial step in z-direction	m
ϵ	Pipe roughness	mm
λ	Friction factor	–
μ_{area}	Fraction flow area	–
ν	Kinematic viscosity of a fluid	m^2/s
ρ	Density	kg/m^3
ρ_f	Density of fluid	kg/m^3
ρ_i	Density of the mixture in the i$^{\text{th}}$ element	kg/m^3
ρ_m	Density of mixture	kg/m^3
ρ_s	Density of solid $2650\,\text{kg/m}^3$	kg/m^3
ρ_w	Density of water $1025\,\text{kg/m}^3$	kg/m^3
$\frac{\epsilon}{D}$	Relative pipe roughness	–
τ_m	Mixture shear stress	Pa
θ	Overlap fraction of the buckets	–
φ	Angle of inflow gap	rad

ζ_{Carnot} Carnot loss coefficient   –

Roman Symbols

Symbol	Description	Unit
A_1	Upper area of the element	m^2
A_2	Lower area of the element	m^2
A_3	Area of the water in or outflow	m^2
C	Chezy coefficient	–
c_d	Drag coefficient	–
D	Diameter of the fallpipe	m
d	Diameter of the sphere	m
D_{low}	Lower diameter of the bucket	m
D_{mean}	Mean diameter of the bucket	m
D_{up}	Upper diameter of the bucket	m
F_b	Buoyancy force	N
F_d	Drag force	N
F_g	Gravitational force	N
F_x	Forces acting in x-direction	N
F_z	Forces acting in z-direction	N
F_{Carnot}	Carnot forces	N
$F_{viscous}$	Viscous forces	N
g	Gravitational acceleration	m/s^2
i_{max}	Location of last element	–
i_{max}	Number of last element	–
K	Total number of fractions	–
k	kth fraction	–
L_{bucket}	Length of the bucket	m
m	Mass	kg
n	Number of elements	–
O	Wet surrounding area the fallpipe	m
P	Production	kg/s
p	Pressure	Pa
p^*	Intermediate pressure	Pa
p_e	External pressure source	Pa
Q_i	Volume flow rate in the ith element	m^3/s

Q_s	Volume flow rate of solids	kg/m^3
$Q_{in,i}$	Volume inflow rate in the ith element	m^3/s
Re	Reynolds number	−
Re_p	Particle Reynolds number	−
S	Source or sink term	−
S_1	Top surface of element	m
S_2	Bottom surface of element	m
S_2	Inflow surface of element	m
Stk	Stokes number	−
V	Volume of element	m^3
v	Velocity	m/s
v_f	Velocity of the fluid	m/s
v_m	Mixture velocity	m/s
v_{fall}	Fall velocity of rock (settling + mixture)	m/s
v_{flow}	Velocity of in- or outflow of the element	m/s
w_s	Settling velocity of a particle	m/s
$w_{e,p}$	Terminal settling velocity corrected for fallpipe influence	m/s
w_e	Equilibrium settling velocity of rock	m/s
$w_{he,p}$	Hindered settling velocity of rock corrected for pipe influence	m/s
w_{he}	Hindered settling velocity	m/s
$w_{r,k}$	Settling velocity of fraction with respect to liquid phase	m/s
$w_{sm,k}$	Settling velocity of fraction with respect to the mixture velocity	m/s

List of Figures

List of Tables

1

Introduction

This chapter includes an overview of the report. Firstly, a general introduction of the subject will be given. Secondly, the motivation of this thesis will be described in the problem definition and the thesis objective. Thirdly, the approach of this thesis will be discussed and finally, the outline of this report will be given.

1.1. GENERAL INTRODUCTION

Subsea rock installation is used for various kinds of applications. Pipeline protection, scour protection, upheaval buckling, insulation, pipeline crossings and pre-lay seabed preparation are some examples where rock installation can be applied.

For rock installation generally two types of vessels can be used namely: a side stone dumping vessel or a fallpipe vessel. Commonly a side stone dumping vessel will be used in shallow waters up to 50m of water depth whereas fallpipe vessels can be used in water depths up to 1200 meters. A disadvantage of a side stone vessel is that while dumping rocks, spreading of the rocks will occur because of underwater currents and lift forces acting on the rocks. The spreading of the rocks results in less accurate rock placement, which is why in deeper water, rocks will be guided by a fallpipe to the sea bottom to increase the accuracy.

A second reason for using a fallpipe is to increase the total fall velocity of the rocks because a mixture flow will be generated in the fallpipe. There are two commonly used fallpipe systems in the offshore industry. Whereas other dredging companies are making use of a closed fallpipe system, Van Oord uses a semi-closed fallpipe, which is built up from open-ended buckets. The two fallpipe systems can be seen in figure 1.1.
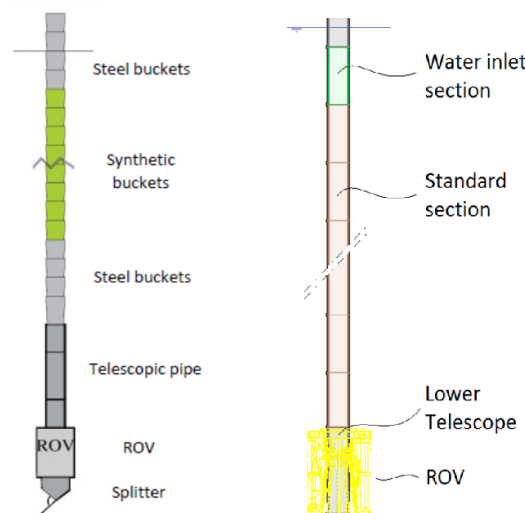
Figure 1.1: Semi-closed and closed fallpipe systems

The main difference between the two fallpipe systems is that by a semi-closed fallpipe the water can freely

flow in and out of the fallpipe if there is a pressure difference between the in and outside of the fallpipe. While for a closed fallpipe a specific inlet section is placed in the fallpipe. At that inlet location water can flow into the fallpipe when there is an under pressure in the pipe. The area of the opening can be adjusted so the total amount of water flowing into the fallpipe can be controlled. At the lower end of both fallpipe systems a remotely operated vehicle (ROV) is placed. The main function of the ROV is controlling the fallpipe and next to that cameras at the ROV will give a better view of what happens at the sea bottom.

1.2. PROBLEM DEFINITION

Scarcity of energy resources drives mankind further offshore and towards deeper waters. Protection of subsea infrastructure is of eminent importance in these environments. The key parameter to have a good control on the installation of rocks is the falling time. For larger water depths up to 1200 meters, the accuracy of the falling time prediction becomes more important because a small deviation can result in a large difference between prediction and reality. Resulting in production losses and off target subsea installation work. This means knowledge of the falling time i.e. the time it takes before a specific input production comes out at the lower end of the fallpipe becomes more and more important for optimizing the subsea rock installation process. In a fallpipe the total fall velocity of the rocks is a combination of the settling velocity of the rock and the flow in the fall pipe, which is driven by the density difference between the stone-water mixture in the pipe and the ambient water. The flow in the fall pipe is a large contributor to the total fall velocity and depends on the density change in the fall pipe. Especially during start-up phase and production changes, when the mixture velocity changes, it is of special interest. When the fall process of rock in a fallpipe is better understood, a better estimation of the falling time can be made.

The problem definition is as follows:

> *" There is a limited extent of knowledge about the falling time of rock during subsea rock installation, especially due to the start-up phase of the mixture velocity in the fallpipe."*

1.3. THESIS OBJECTIVE

The process of rock installation can be divided into two main parts. The first part is the process inside the fallpipe. The second part is the process when the rocks are leaving the fallpipe and the interaction with the seabed. A lot of research is already carried out regarding the process from the end of the fallpipe till the sea bottom by e.g. [Ravelli, 2012], [Kevelam, 2016] and [Reus, 2004]. Less is known about the process in the fallpipe. Therefore, this thesis will focus on the first part of the rock placement process, which is the fall process of the rocks in the fallpipe. The main objective is to gain a better understanding of the processes occurring in the fallpipe during rock dumping by developing an one dimensional model to predict the falling time of the rocks.

The main objective of this thesis is:

> *"Develop a model to predict the falling time, concentration profile in the fallpipe and outlet velocity for a semi-closed fallpipe during subsea rock installation"*

1.4. THESIS APPROACH

The approach of this thesis can be divided into two parts. First a literature study is carried out to get more insight in the state-of-the-art knowledge of subsea rock installation and to get familiar with the processes involved. The second part focuses on the modelling of the fall process of rock in a numerical model. To check if the model gives a representative outcome of the real process, the outcome will be validated by in situ measurements. An overview of the approach is given in figure 1.2.
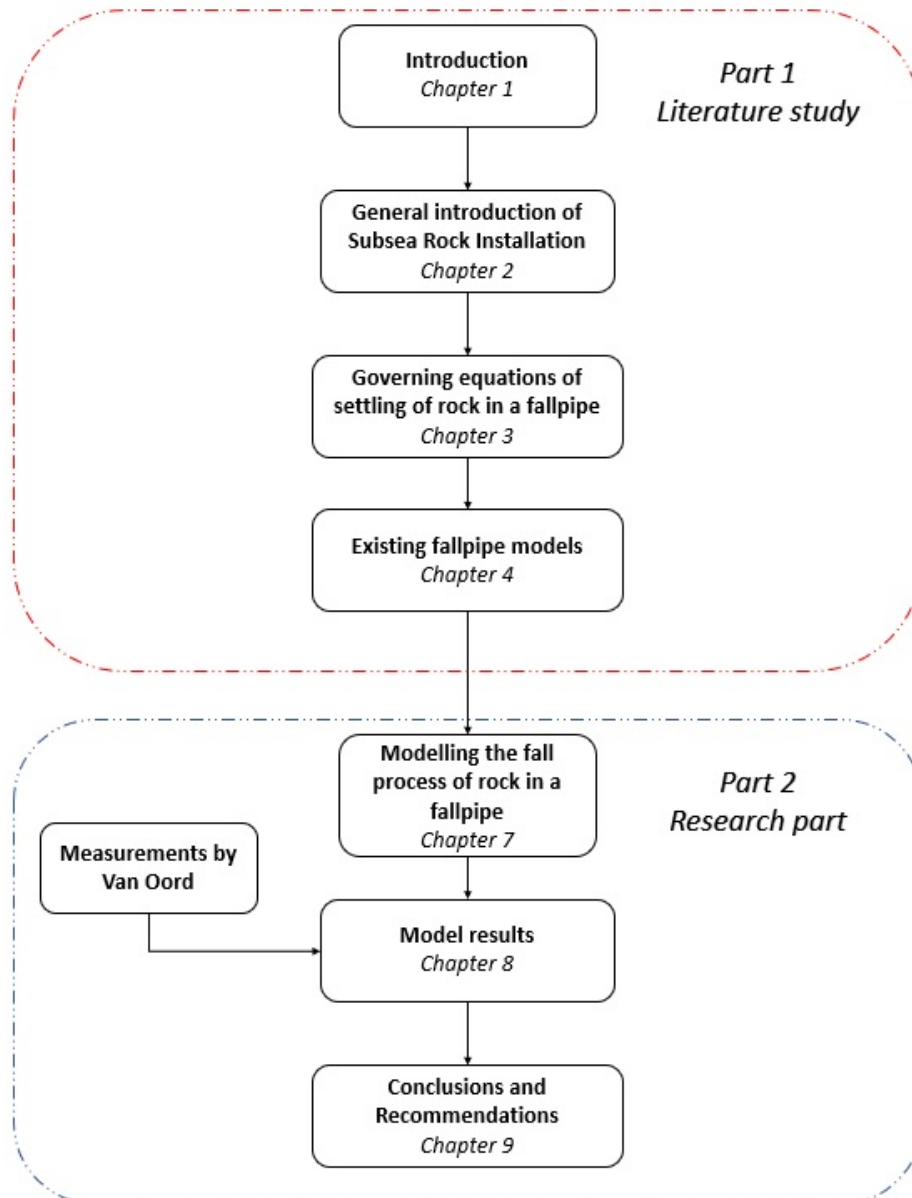
Figure 1.2: Overview of thesis approach

1.5. REPORT OUTLINE

This reports is divided into two parts. The first part focuses on familiarization with the process of subsea rock installation and giving an overview of the current calculation models. This will includes chapter 2 to 5. The second part focuses on the modelling of the fall process and includes chapter 6 to 9.

Part I

- **Chapter 2: Subsea Rock Installation:** An overview of rock placement operation is given and the working of a fallpipe vessel used by Van Oord will be described.

- **Chapter 3: Settling of rock:** An overview of the forces acting on a rock, while settling is explained and some background is given about the settling of rocks.

- **Chapter 4: Modelling of rocks in a fallpipe:** An overview of the models which are used for subsea rock installation during the years is given.

- **Chapter 5: Concluding remarks literature study:** A summary of the literature study is given.

Part II

- **Chapter 6: Introduction to the research:** An introduction of the research will be described.

- **Chapter 7: Model description:** The built up of the model will be discussed.

- **Chapter 8: Model results and case study:** An overview of the results of the model for different cases is given and compared with experimental data by Van Oord.

- **Chapter 9: Final conclusions and recommendations:** Concluding remarks and recommendations for further work.

"On the fall process of rock during Subsea Rock Installation"

Master thesis

Part I

Literature Study

2

Subsea Rock Installation

In the offshore industry, rock dumping is used for different kind of applications. In the early years it was especially used for making dikes and breakwaters. Nowadays the name rock dumping changed in subsea rock installation due to the implementation of new technologies and increasing difficulties of the projects. In the first part of this chapter an overview of the different rock placement operations will be given. The second part will give an introduction of what kind of vessels can be used and finally the working of the by van Oord used vessel "The Nordnes" will be described.

2.1. ROCK PLACEMENT OPERATIONS

Subsea rock installation can be used in a large variety of offshore projects. A view examples, where subsea rock installation can be applied are briefly described in this section.

2.1.1. PIPELINE PROTECTION

Pipelines at the sea bottom should be protected against dragging anchors and fishery in areas where a lot of sea-going activities takes place. The anchors and fishing nets can cause damage to the pipeline. In order to prevent this, rocks are placed over the pipeline, as shown in figure 2.1. It is important that the size of the rocks are smaller than the mesh size of the fishing net, so the nets will not take the rocks away from the pipeline and the protection stays in place.

2.1.2. SCOUR PROTECTION

Waves and currents can cause erosion of the seabed around fixed structures e.g. oil platforms and monopiles used for offshore wind turbines. This is called scour. The sand around the structures can be washed away due to currents, resulting in an stability decrease of the foundation. To prevent against scouring, rocks are installed around the structure, as displayed in figure 2.2.
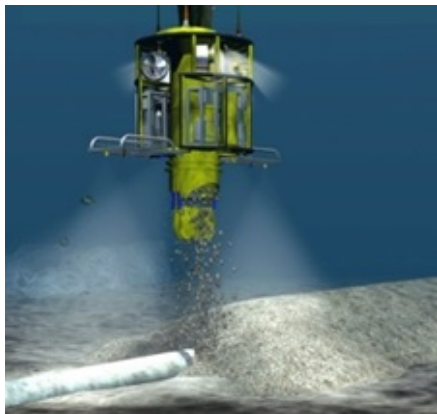
Figure 2.1: Pipeline protection

Figure 2.2: Scour protection

2.1.3. Pipeline crossing

When laying new pipelines it can be necessary to cross earlier laid pipelines. This can be done by making a berm over the old pipeline as shown in figure 2.3. The rock berm will perform a gentle slope over the old pipeline to make sure there will be no high tensions in the new-laid pipeline.

2.1.4. Pre-lay seabed preparation

The sea floor is not flat, which means before placing structures or pipelines at the sea floor sometimes seabed preparations should be carried out. Where the sea floor is not flat rocks are placed to level out the seabed so a structure can stand on it or for decreasing the free span of a pipeline as displayed in figure 2.4.
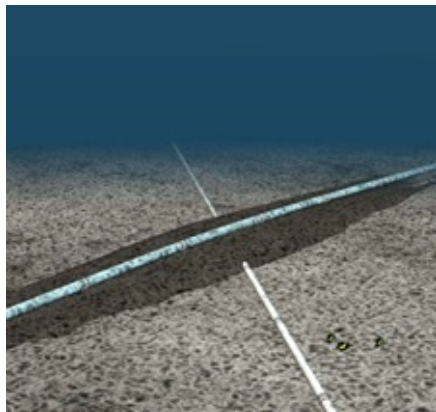
Figure 2.3: Pipeline crossing
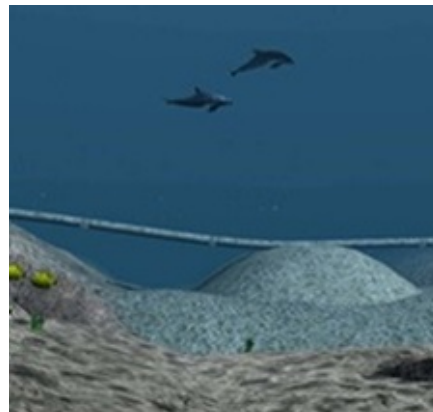
Figure 2.4: Freespan correction

2.2. Side stone dumping vessels

A side stone dumping vessel is mostly used when rocks are installed in shallow water. When rocks are dumped in water spreading will occur because of horizontal forces and/or currents. When side dumping will be applied in deeper water the accuracy will decrease. That is why this technique is commonly used for the construction of breakwaters in shallow water.

2.3. Fall pipe vessels

For installing rocks in deeper water, two types of fall pipe systems can be used, namely a closed fallpipe and a semi-closed fallpipe. The fallpipe will guide the rocks to the sea bottom to increase the accuracy. By using a fallpipe system, a mixture flow will be generated when water starts flowing into the fallpipe. This flow will increase the total fall velocity of the rock.

2.3.1. Closed fallpipe

A closed fallpipe consists of multiple standard sections which are mounted on top of each other. At the top end a water inlet section is placed. This section is used to control the inflow of water in the pipe. If there is no inflow of water in the fall pipe, the water level in the pipe will drop when the process of rock dumping starts. An overview of the water level drop can be seen in figure 2.5. This is because of the density increase of the mixture in the fall pipe, which results in a higher pressure. Based on the Bernoulli equation this results in an outflow at the end of the fallpipe. For deeper waters, if the water level drops too far, a large difference between inner and outer pressure of the fallpipe can occur. Due to these high pressure differences a pipeline can collapse. This is one of the reason why for a closed fallpipe a water inlet segment is installed at the top end of the fallpipe, to ensure the water level will not drop to far and for controlling the flow in the fallpipe.
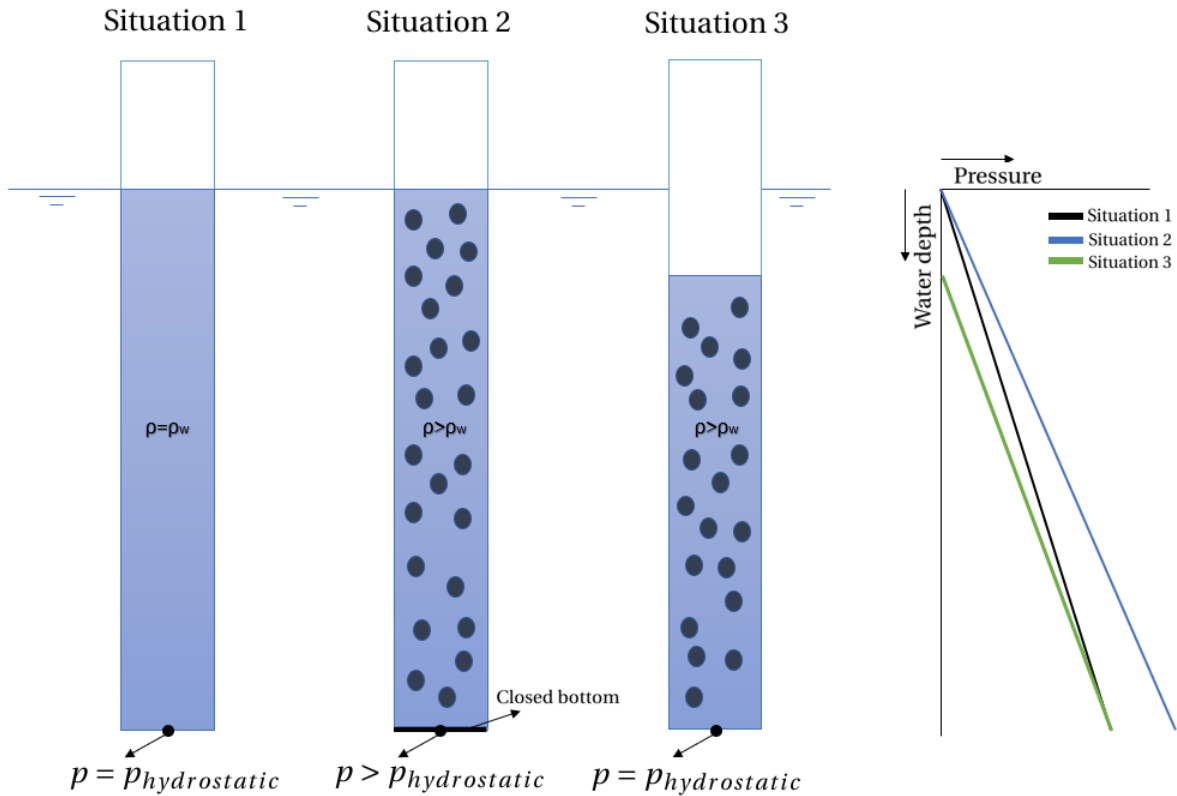
Figure 2.5: Overview of water level drop in a closed fallpipe with pressure profile

For example, a 700m long fallpipe with a concentration of 5 % will experience a pressure at the end of the pipe because of the hydrostatic column of 7.6 MPa. While the surrounding pressure is 7.0 MPa. To level this out the water level in the fallpipe will drop 55.52 m.

2.3.2. Semi-closed fallpipe
The system used by van Oord is an open construction consisting of multiple open-ended buckets. The buckets at the upper and lower end of the fallpipe are made of steel and the buckets in the midsection are made of synthetic material. Multiply buckets are connected by two steel chains which is called a string. By connecting multiple strings a total depth of 1200m can be realized. At the lower end of the fallpipe a Remotely Operated Vehicle (ROV) is attached. Because of the ROV, the rocks can be placed more accurate as the position of the lower end of the fallpipe can be controlled form the control room in the vessel.

2.4. Fallpipe vessel: "The Nordnes"
The Nordnes is one of the fallpipe vessels of Van Oord. The total length of the vessel is 166.70m with a span of 26.23m. The Nordnes can carry 26,238 tons and has a maximum rock installation capacity of 2000 tonnes per hour. In figure 2.6 a cross section of "The Nordnes" is given.

The dumping process
Before the process of dumping rocks starts the fallpipe should be launched. The fallpipe consists of multiple strings with buckets, which are all stored at the ship. Firstly the ROV is launched through the moonpool. When the ROV is launched the buckets will follow up by using the bucket winch, see figure 2.7. The first part of the fallpipe is a telescopic pipe, which can be used to follow the seabed without the need of extra buckets. On top of the telescopic pipe a couple of steel buckets will be placed. The midsection of the fallpipe is made of synthetic buckets and the last view meters to the ship is made of steel buckets again. The lower end and upper end of the fallpipe are made of steel buckets because higher forces and stress levels will occur at these parts of the fallpipe. An overview of the structure of a fallpipe can be seen in figure 2.8. When the fallpipe is in place the dumping process can start.
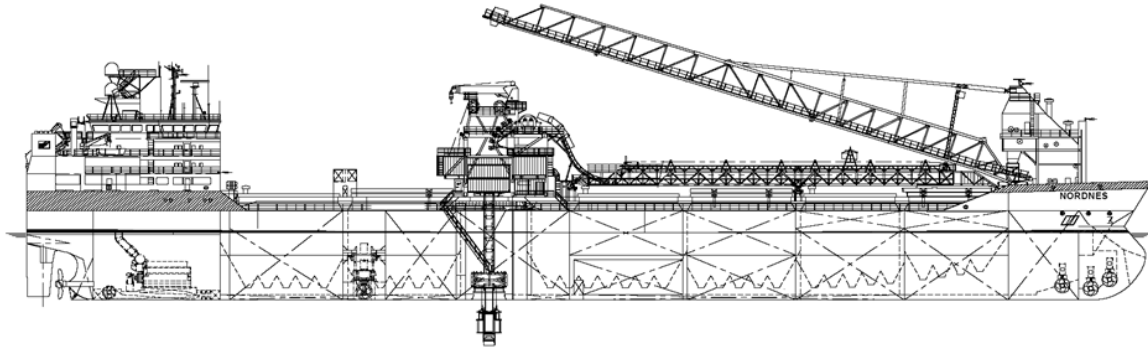
Figure 2.6: Cross section of the Nordness
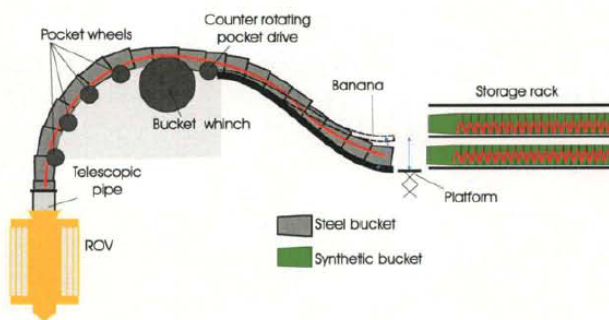
Figure 2.7: Bucket launching system
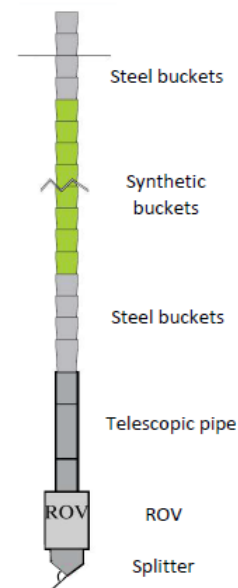
Figure 2.8: Built up of a semi-closed fallpipe

Transport of the rocks to the fallpipe

The route of the rocks will be described step by step and a complete overview of the route is given in figure 2.9.

(i) The rocks are all stored in the holds of the ship. The main conveyor belt is at the bottom of the hold and transports the rocks to the front of the ship. The transport of rock can be controlled by adjusting the speed of the conveyor belt.

(ii) At the front of the vessel a C conveyor, a sandwich of two belts with the rock in the middle, deposits the rock on too the boombelt.

(iii) The boombelt above deck, transports the rocks from the front of the ship to the hopper.

(iv) From the hopper, the rocks will be transported by conveyor belts to the moonpool and via the feeder the rock is transfered to top steel bucket and down into the fallpipe. The production output is controlled by adjusting the speed of the conveyor belts.
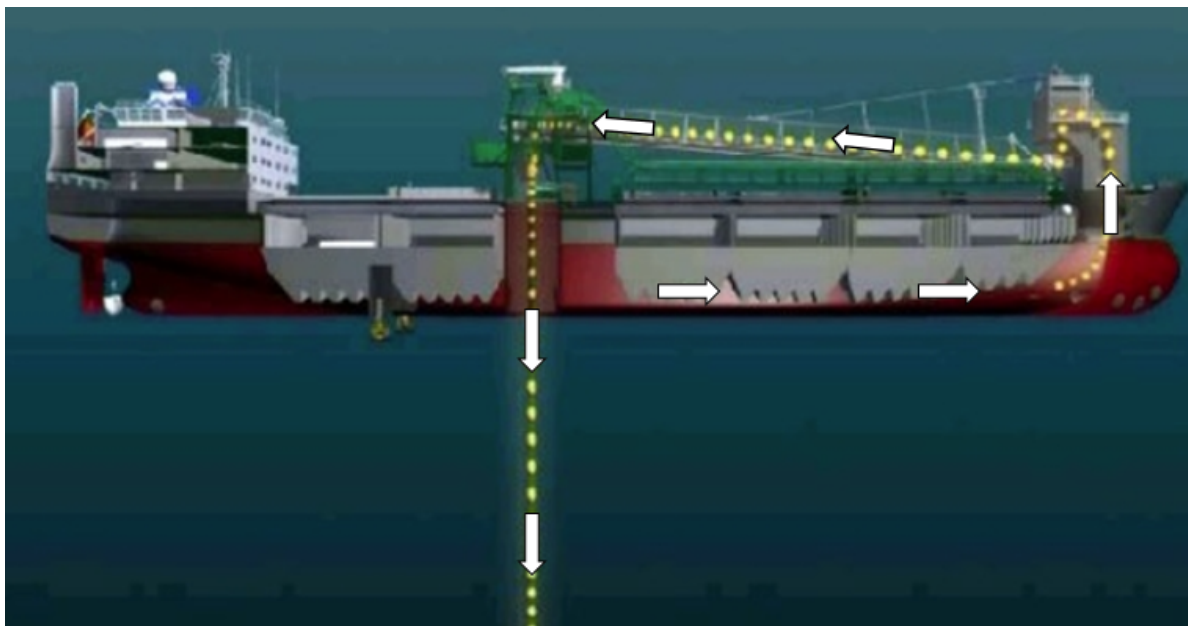
Figure 2.9: Transport route of rocks

Buckets
The buckets which are used for the fallpipe are made of steel or synthetic material. The first and last part of the fallpipe are both made of steel because of its resistance to wear.The synthetic buckets are used to reduce to overall weight on the chains and span the major part of the fallpipe. The diameter of the buckets determines the maximum allowable diameter of the rocks. The lower diameter of the bucket is 849mm and the upper diameter is 1097mm. The height of a bucket is 2225 mm.

Remotely Operating Vehicle (ROV)
The Remotely Operating Vehicle is at the lower end of the fallpipe. This is the only part of the fallpipe which is controllable. The ROV is hanging on the vessel with three cables and the telescopic pipe of the fallpipe is connected to the ROV, which means the rocks are falling through the ROV. To provide the ROV and other equipment with power there are umbilicals form the vessel to the ROV.

2.5. CONCLUSION
Subsea rock installation is applied in different offshore projects. There is a difference between rock installation in shallow water and deeper waters. By using a fallpipe vessel rocks can be installed more precise because spreading will only occur at the last several meters to the sea floor, when the rocks are not in the fallpipe any more. In the offshore industry two different kind of fallpipe systems are used, namely a closed fallpipe and a semi-closed fallpipe. For a closed fallpipe there is a water inlet at the top end of the fallpipe to control the water level in the fallpipe, while for a semi-closed fallpipe the water can freely flow in or out of the fallpipe through the openings between the buckets.

3

Terminal settling velocity of rock

In this chapter the settling of rocks will be evaluated. First the settling of a single rock will discussed. Followed by the influence of multiple rocks settling at the same time will be described and finally the fallpipe influence on the settling velocity will be described.

3.1. TERMINAL SETTLING VELOCITY OF A SINGLE ROCK

The terminal settling velocity depends on the forces acting on a particle. When the forces are in equilibrium the terminal settling velocity is reached.

Forces acting on rock

The dumping of a single rock can be described as follows. When a particle is falling in water, there are three forces acting in vertical direction on the particle namely: Gravitational force (F_g), buoyancy force (F_b) and drag force (F_d).

Gravitational force

The gravitational force can be determined by using the following formula:

$$F_g = mg \tag{3.1}$$

Where F_g is the gravitational force, g is the gravitational acceleration and m is the mass of the object. The mass of the object is considered as a sphere and can be calculated by the following formula:

Figure 3.1: Vertical forces acting on a particle

$$m = \frac{\pi}{6}d^3\rho_s \tag{3.2}$$

Where d is diameter of the sphere and ρ_s is the density of the solid.

Buoyancy force

The buoyancy force is acting on the particle in opposite direction of the gravitational force and can be calculated by the following formula:

$$F_b = \frac{\pi}{6}d^3\rho_f g \tag{3.3}$$

F_b is the buoyancy force and ρ_f is the density of fluid.

Drag force

The drag force is also acting on opposite direction of the gravitational force and can be calculated by:

$$F_d = \frac{1}{2}C_d\rho_f w_s^2 \tag{3.4}$$

Where F_d, C_d and w_s are respectively the drag force, drag coefficient and the terminal settling velocity of a single particle in still water.

Drag coefficient

During the years a lot of research has been done to determine an accurate expression for C_d for perfect spheres over the entire particle Reynolds number (Re$_p$) regime. At higher Reynolds numbers separation of the boundary layer will occur and a wake will form. This means a pressure difference between the front and the rear of the object will occur. The drag coefficient can be calculated by using the particle Reynolds number. Three different regimes can be distinguished: the laminar, turbulent and transition regime. For each regime a different relation applies [Van Rhee, 2017]:

Table 3.1: Drag coefficient based on particle Reynolds number

$Re_p < 1$	$C_d = \frac{24}{Re_p}$
$1 < Re_p < 2000$	$C_d = \frac{24}{Re_p} + \frac{3}{\sqrt{Re_p}} + 0.34$
$Re_p > 2000$	$C_d = 0.4$

The Reynolds particle number (Re$_p$) is defined as:

$$Re_p = \frac{w_s d}{\nu} \tag{3.5}$$

Where ν is the kinematic viscosity of the fluid. The particle Reynolds number depends on the fall velocity of the particle. The set of equation 3.1-3.5 can be solved iteratively to find the terminal settling velocity.

Calculations fall velocity

The fall velocity of the particle can be calculated by using the second law of Newton:

$$F_z = ma \tag{3.6}$$

Where F_z is the summation of the forces acting in the z-direction and a is the acceleration in z-direction. By filling in equations 3.1, 3.3 and 3.4 into Newton's law of motion. The settling velocity with respect to distance [Miedema, 1981] and time can be derived. The equations respect to time and distance are given in equation 3.7 and 3.8. Note: In equation 3.7-3.9 and figure 3.2-3.3, the drag coefficient is constant, where actually the drag coefficient is a function of the particle Reynolds number. To provide a general insight of the distance and time needed to reach the terminal settling velocity, it is chosen to use a constant value for the drag coefficient.

$$w_s(z) = \sqrt{\frac{4g(\rho_s - \rho_f)d}{3\rho_f C_d}\left(1 - e^{\frac{-3\rho_f C_d z}{2\rho_s d}}\right)} \tag{3.7}$$

The exponential in the second part of the formula represents the start of the falling particle. When the distance (z) goes to infinity, the exponential will go to zero and the particle will reach its equilibrium velocity.

$$w_s(t) = \sqrt{\frac{4gd(\rho s - \rho_f)}{3C_d \rho_f}} tanh\left(\sqrt{\frac{3C_d g \rho_f}{8d(\rho_s - \rho_f)}}t\right) \tag{3.8}$$

After a certain distance and/or time the forces will be in equilibrium which will result in a constant velocity. The equilibrium velocity can be calculated by the following equation:

$$w_s = \sqrt{\frac{4gd(\rho_s - \rho_f)}{3C_d \rho_f}} \tag{3.9}$$
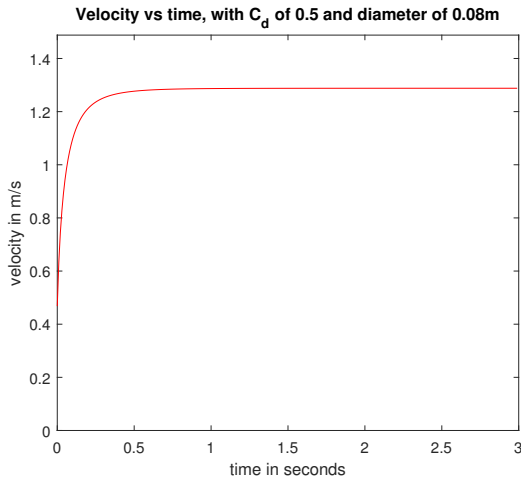
Figure 3.2: Velocity profile of a settling sphere as function of time
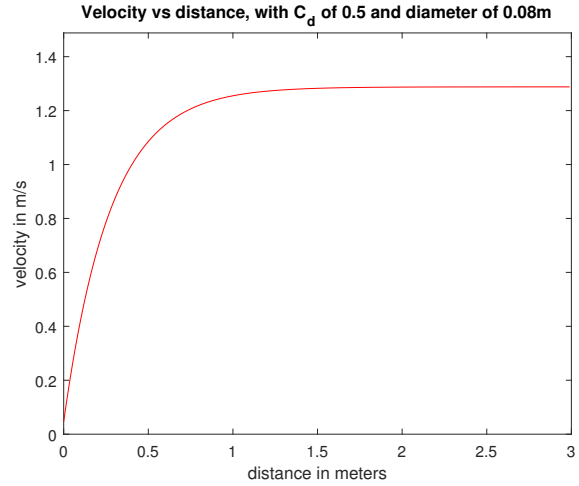
Figure 3.3: Velocity profile of a settling sphere as function of distance

In figure 3.2 and 3.3, it can be seen that it will not take a lot of time and/or distance to reach the equilibrium velocity. So it is reasonable to say that in a fallpipe, the rocks will reach their equilibrium settling velocity instantaneously because the falling distance to reach the equilibrium velocity is small compared to the total length of the fallpipe. Note that figure 3.2 and 3.3 are generated with a fixed drag coefficient to provide insight of distance and time needed to reach the terminal settling velocity. To be more precise the particle Reynolds number should be implemented in the drag coefficient.

Ferguson and Church

The force balance, which was described in the previous section, is more complex to use because of the drag coefficient which depends on the particle Reynolds number. In 2004, Ferguson and Church developed an empirical relation for the settling velocity, based on the experiments of Richardson and Zaki [1954], which does not include the drag coefficient [Ferguson & Church, 2004]:

$$w_e = \frac{\Delta g d^2}{C_1 \nu + \sqrt{0.75 C_2 \Delta g d^3}} \tag{3.10}$$

Where C_1 and C_2 are respectively 18 and 1 for natural sands and Δ is the relative density and can be determined by using the following formula:

$$\Delta = \frac{\rho_s - \rho_f}{\rho_f} \tag{3.11}$$

An advantage of the equation founded by Ferguson and Church is, there is no need to use an iteration scheme to determine the correct drag coefficient. When comparing Newton's law and the equation of Ferguson and Church it can be seen that the same results are obtained, as shown in figure 3.4. A typical rock diameter for subsea rock installation is in the range of 22-125mm.

3.2. SETTLING OF MULTIPLE ROCKS

In the previous section the fall process of a single rock and the forces acting on the rock are described. During subsea rock installation multiple rocks are dumped at the same time. The behaviour of rocks in groups is described in this section.
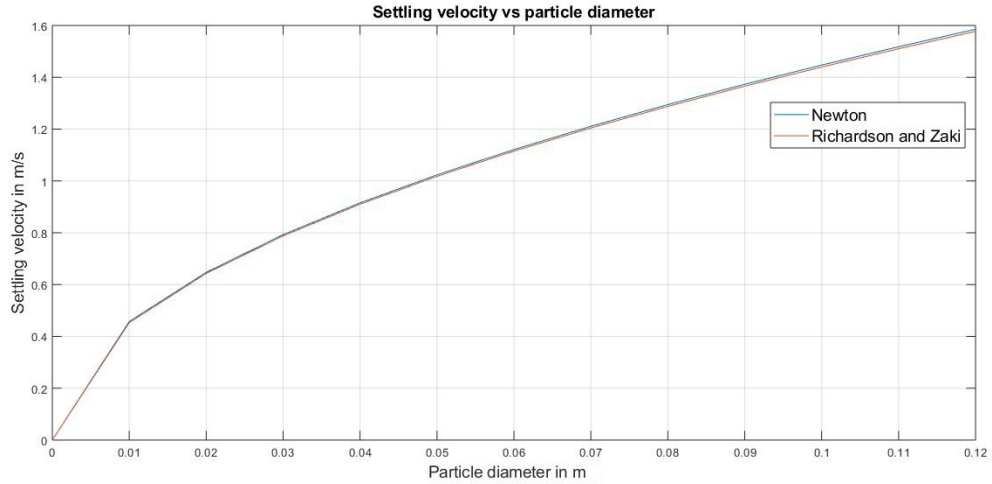
Figure 3.4: Settling velocity for a range of particle diameters

While rocks are settling in a group they will have some influence on each other this is called hindered settling. Over the years, research has been done by various researchers. A series of experiments on hindered settling were carried out by Richardson and Zaki in 1954 and they developed an empirical relation [Richardson & Zaki, 1997] to take into account the hindered settling based on their experiments:

$$w_{he} = w_e(1 - \alpha_s)^n \tag{3.12}$$

Where w_{he} is the hindered equilibrium velocity, α_s is the concentration of solids and n is the empirical exponent related to the particle Reynolds number (Re_p). The particle Reynolds number can be calculated by equation 3.5. The empirical exponent n can be calculated by using the following formula [Rowe, 1987]:

$$n = \frac{4.7\left(1 + 0.15Re_p^{0.687}\right)}{1 + 0.253Re_p^{0.687}}. \tag{3.13}$$

Equation 3.13 covers the empirical exponent n for all ranges of the particle Reynolds number. Richardson and Zaki developed different formulas to calculate the exponent n for different ranges of particle reynolds numbers, which can be seen in table 3.2[Rook, 1994]. Comparing the different ways for calculating the exponent based on the particle Reynolds number, it can be seen that equation 3.13 will give good results for the whole range of particle Reynolds numbers. Where $\frac{d}{D}$ is the ratio between particle diameter and pipe diameter.

Table 3.2: Hindered settling factor

$n = 4.65 + 19.5\frac{d}{D}$	for $Re_p < 0.2$
$n = (4.35 + 17.5\frac{d}{D})Re_p^{-0.03}$	$0.2 < Re_p < 1$
$n = (4.45 + 18.5\frac{d}{D})Re_p^{-0.1}$	$1 < Re_p < 200$
$n = 4.45Re_p^{-0.1}$	$200 < Re_p < 500$
$n = 2.39$	$Re_p > 500$

According to [Wijk, 2011] equation 3.13 still holds for coarse gravel (high $\frac{d}{D}$) and a value of n=2.4 was found during fluidization experiments [Van Rhee, 2017].

3.3. FALLPIPE INFLUENCE
The presence of the fallpipe will have influence on the settling velocity of the particles. The settling velocity of a particle can be calculated by Newtons equation in turbulent regions [Li *et al.*, 2014], given as follows :

$$w_{he,p} = w_{he}\left(1 - \left(\frac{d}{D}\right)^2\right)\sqrt{\left(1 - 0.5\left(\frac{d}{D}\right)\right)} \tag{3.14}$$

Where $w_{he,p}$ is the settling velocity in the pipe, d is the particle diameter and D is the diameter of the fallpipe.

Looking at equation 3.14 and figure 3.5 it can be seen that, when the diameter of the rock increases, the settling velocity decreases. For small diameter particles the fallpipe will have no influence on the settling velocity but during subsea rock installation relatively larger particles with respect to the fallpipe diameter are used, so there will be some reduction on the settling velocity for these particles.
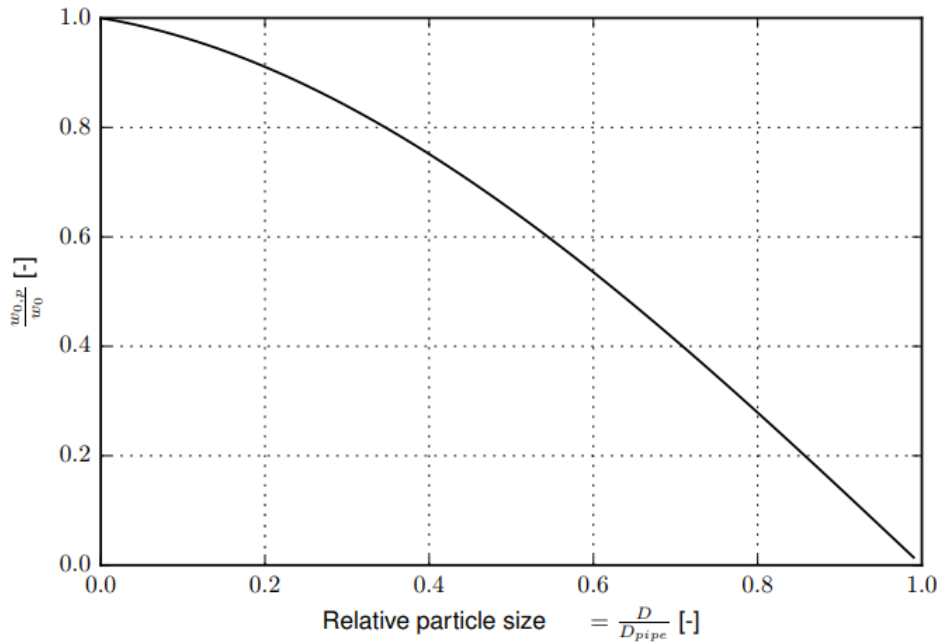
Figure 3.5: Wall influence on the settling of a particle

3.4. CONCLUSION

The settling velocity can be determined by calculating the forces acting on the rock during falling. For this technique a drag coefficient is needed, which is difficult to determine for rocks due to the particle Reynolds number. Richardson and Zaki developed a different formula to determine the settling velocity, which does not include the drag coefficient. When a comparison is made between the different methods, there is shown that both methods obtain almost the same settling velocity.

During subsea rock installation multiple rocks are dumped at the same time, this results in interaction between the rocks. The settling velocity will decrease if the concentration increases.

While rocks are settling in a fallpipe, the fallpipe will have some influence on the settling velocity as well. The reduction of the settling velocity due to the fallpipe depends on the relative particle size.

4

Modelling of rocks in a fall pipe

In this chapter, an overview is given of the fallpipe models conducted over the years. First the static models for subsea rock installation will be discussed followed by the dynamic models. The static models only look at a specific moment in time or calculate an equilibrium velocity, while the dynamic models take the concentration development into account. Finally, a drift-flux model is discussed which is applied in the deep sea mining industry for transporting manganese modules.

4.1. Static models for subsea rock installation

4.2. Dynamic models for subsea rock installation

4.3. Vertical hydraulic transport for deep sea mining

In 2011 research has been carried out into flow assurance for vertical hydraulic transport for deep sea mining [Wijk, 2011]. Some similarities can be seen between SRI and deep sea mining, that is why an overview of this model will be given here. The focus of the research was on the possibility of blockage while transporting manganese nodules from the sea bottom to the surface. The transport of the modules is computed by solving the advection-diffusion equation for the individual fractions using a drift-flux model. The drift-flux model models the water and the manganese nodules as a mixture with a certain density(ρ_m) and corrects for the slip velocity (velocity difference between mixture and solids). The continuity equation is written as function of density while van Es wrote it as function of concentration solids. The continuity equation for a constant in and outflow area is given as follows:

$$\frac{\partial \rho_m}{\partial t} + \frac{\partial (\rho_m v_m)}{\partial z} = 0 \tag{4.1}$$

The density change in time depends on the net density flux of the element. To calculate the mixture velocity for the new time step the conservation of momentum in z-direction is given by[Wijk, 2011]:

$$\underbrace{\frac{\partial (\rho_m v_m)}{\partial t}}_{\text{Velocity change in time}} + \underbrace{\frac{\partial (\rho_m v_m^2)}{\partial z}}_{\text{Momentum flux}} = \underbrace{\frac{\partial p}{\partial z}}_{\text{Pressure gradient}} - \underbrace{\frac{4\tau_m}{D}}_{\text{Viscous stresses}} - \underbrace{\rho_m g}_{\text{Gravity force}} \dots$$

$$+ \underbrace{\sum \frac{\partial p_e}{\partial z}}_{\text{External pressure gradient}} \underbrace{- \frac{\partial}{\partial z}\Big((1-c_v)\rho_f(v_m - v_f)^2 + \sum_{k=1}^{K} c_{v,k}\rho_{s,k}(v_m - v_{s,k})^2\Big)}_{\text{Correction for slip velocity}} \tag{4.2}$$

Note that the momentum equation is divided by the control volume (V). For the viscous term it is clarified in the following equation:

$$F_{viscous} = \frac{\pi D \Delta z \tau_m}{\frac{\pi}{4} D^2 \Delta z} = \frac{4\tau_m}{D} \tag{4.3}$$

Where τ_m is the shear stress of the mixture, D is the diameter of the pipe and Δz is the height of the element. The total solid input phase is divided into number of K fractions depending on particle diameter. Each fraction has its own settling velocity $w_{he,p,k}$, density $\rho_{s,k}$ and volume fraction $c_{v,k}$. Important to notice is that the settling velocity will decrease the solids velocity in deep sea mining while for SRI the settling velocity will increase the solids velocity. The solids velocity can be calculated by using the following formula:

$$v_{s,k} = v_m - w_{he,p,k} \tag{4.4}$$

When the solids velocity (v_s) is calculated the transport of the solid fractions is described by the advection diffusion equation (4.5). This will give a concentration and velocity profile in the riser.

$$\underbrace{\frac{\partial c_v}{\partial t}}_{\text{Concentration change in time}} + \underbrace{\frac{(\partial c_{v,k} v_{s,k})}{\partial z}}_{\text{Advection term}} = \underbrace{\frac{\partial}{\partial z}\left(\epsilon_z \frac{\partial c_{v,k}}{\partial z}\right)}_{\text{Diffusion term}} \tag{4.5}$$

Where the diffusion term depends on the diffusion coefficient (ϵ_z), which depends on the Stokes number given by the following equation:

$$Stk = \frac{4(\rho_s - \rho_f)d|v_m|}{3\rho_f D w_{he,p} C_d} \tag{4.6}$$

For higher Stokes numbers i.e. for larger particle diameters, the diffusion coefficient is set to zero. Hence the influence of the diffusion part will not be taken into account for large particle diameters, which are applied in deep sea mining and SRI.

4.4. CONCLUSION

5

Concluding remarks literature study

In this chapter the main components of the fall process in the fallpipe, which came forward from the literature research are discussed.

- When rocks are settling in water large offsets can occur. This is why in greater water depths, fallpipe vessels are used to guide the settling rocks to the sea bottom. In the offshore industry, there are two commonly used fallpipe vessels namely a semi-open system consisting of multiple open-ended buckets and a closed system built up from pipe segments. When using a fallpipe system during subsea rock installation the fluid in the fallpipe will accelerate and a downwards directed flow will develop in the fallpipe. This results in an additional velocity of the rock, besides the settling velocity. The total fall velocity is a summation of the flow velocity (v_m) and the settling velocity of the rocks (w_s). This velocity will transport the concentration with a higher speed to the end of the fallpipe.

- During subsea rock installation multiple rocks are dumped in the fallpipe at the same time. So a larger number of particles is settling at the same time in the fallpipe and this will effect the settling velocity of the individual particles. When the concentration increases the settling velocity of a single particles decreases. Besides the hindered settling, the fallpipe will have his influence on the settling velocity as well. The reduction of the settling velocity depends on the fraction between the diameter of the particle and the diameter of the fallpipe. If this fraction increases the settling velocity decreases.

- The models, which are used for subsea rock installation at the moment have a strong focus on the settling velocity of the particles, the mixture velocity in the fallpipe or the equilibrium fall velocity of the particles in the fallpipe. To make a better prediction of the falling time of the particles, the start up of the mixture flow should be taken into account and the total fall velocity of the rocks should be a combination of the settling velocity and the mixture velocity generated in the fallpipe. The influence of water in and outflow is highly important because it has effect on the mixture flow in the fallpipe. The mixture flow increases the total fall velocity of the rock and is a significant contributor to this total fall velocity.

- The drift-flux model used by van Wijk will be used to conduct a model for subsea rock installation by using a fallpipe. This model is chosen because it combines the generate mixture flow in the fallpipe and the settling velocity of the rocks, while the other models only uses the mixture flow or settling velocity in the transport equation for the concentration.

On the fall process of rock during Subsea Rock Installation

Master thesis

Part II

Modelling the fall process of rock in a fallpipe

6

Introduction to the research

Rock installation by using a closed or semi-closed fallpipe is applied in various kinds of offshore projects e.g. to protect pipelines and pre- and post-lay seabed preparation. While the offshore industry is moving to deeper waters and the projects become more complex, the accuracy of the falling time prediction becomes more important because small deviations can result in large differences between prediction and reality. The aim of this research is to provide a better understanding of the fall process of rock and to predict the time needed for a specific production rate to reach the end of the fallpipe. The focus of this research will be on the fall process within the fallpipe and specially on the determination of the falling time of the rocks.

6.1. MODEL ASSUMPTIONS
The following assumptions are made in the model:

Assumption 1:
The input of the rocks is modelled as a mixture with a certain density based on the amount of tonnes per hour and the input velocity of the rocks. By using the production and input velocity of the rocks the input concentration (α_{in}), the input velocity (v_{in}) and the density of the input mixture ($\rho_{m,in}$) can be obtained.

Assumption 2:
In chapter 3 the settling velocity as function of distance is discussed. In figure 3.3, it can be seen that the distance to reach the terminal settling velocity is very small in comparison to the total length of the fallpipe. This justifies the assumption that the rocks reach there terminal settling velocity instantaneously when it enters the fallpipe.

Assumption 3:
The input location or upper boundary of the model is fixed. This means that the water level is fixed in the fallpipe. When the water level is fixed, an under pressure in the fallpipe will be generated by the drift-flux model, when the rocks start falling. This under pressure can be rewritten to the water level drop.

Assumption 4:
When there is an overpressure in the fallpipe, the assumption is made that there will only be water flowing out instead of mixture. This assumption is made because this way the maximum flow velocity between the buckets can be determined. If the flow density is equal to the mixture density, the outflow velocities will be lower based on the Bernoulli equation.

6.2. MODEL DEVELOPMENT
In figure 6.1 an overview of the development of the model is given to provide insight of the steps which were taken to develop a representative model for subsea rock installation by using a semi-closed fallpipe. The first step is to model a water flow in the fallpipe, which has been done by using the fractional step method described in chapter 7.2.1. The following step is to model the rocks falling in the fallpipe. This has been done by using the drift-flux model, where the rocks are modelled as a mixture with a certain density based

on the concentration of the rocks and the fluid. The drift-flux model continues on the fractional step method with some extensions. This will be described in more detail in chapter 7.2.1 - 7.2.3. The drift flux model will generate an under pressure in the fallpipe which is equal to the water level drop. In a fallpipe there is the possibility of water in or outflow if there is an under or overpressure. This is modelled in step 3 and is explained in more detail in chapter 7.3. The last step should be taken to create a representative model for a semi-closed fallpipe. In this step the possibility of water in or outflow is modelled for each element depending on an under or overpressure in the fallpipe. This is described in more detail in chapter 7.4.
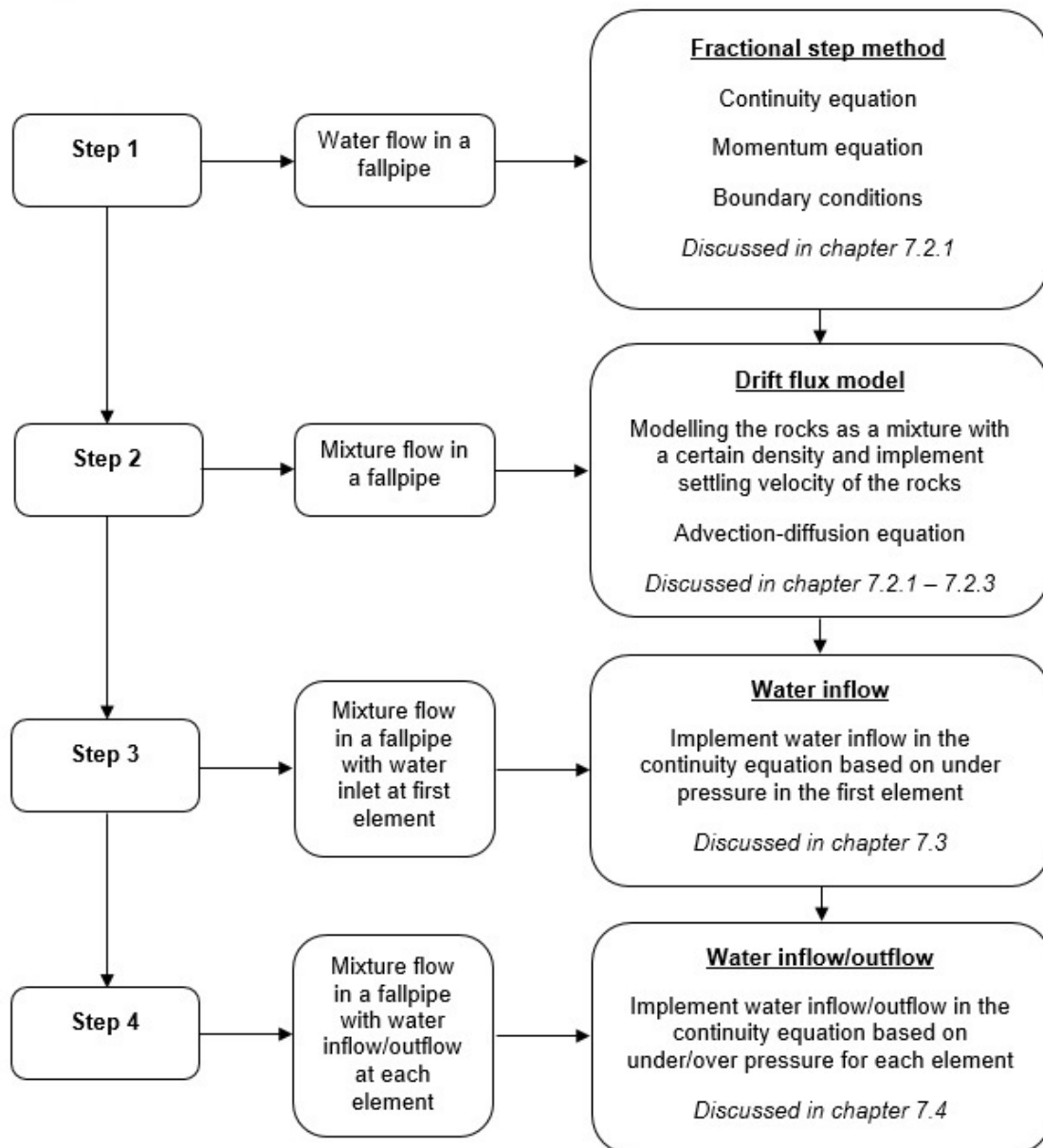
Figure 6.1: Schematic representation of the modelling approach

7

Model description

In this chapter a detailed description of the models is given. First the closed fallpipe model will be discussed followed by the semi-closed model. The mixture flow in the fallpipe is computed by solving the continuity and momentum equations. For both models, the closed fallpipe and semi-closed fallpipe, the drift flux model approach by [Goeree *et al.*, 2016] is used. The settling velocity of rock is calculated by using the hindered settling theory. The transport of solids will be described by the advection-diffusion transport equation.

7.1. CLOSED FALLPIPE MODEL

The model computes the concentration, velocity and pressure profiles in the fallpipe during subsea rock installation in space and time. By doing so the total falling time can be calculated. For obtaining these results, the fallpipe will be modelled as one dimensional with the focus on the z-direction with positive direction upwards.

The total fall velocity of a rock depends on the settling velocity of the rock and the velocity of the mixture (bulk velocity) in the fallpipe. First the mixture velocity will be calculated by solving the Navier Stokes equation, followed by calculating the settling velocity for each fraction with respect to the mixture velocity by taking into account hindered settling. The settling velocity will be added to the mixture velocity and so the total fall velocity of the rock for each fraction is obtained.

Mixture equations

The mixture consist of a solid (rocks) and a carrier liquid. Based on the work of [Jop *et al.*, 2006], the transport of suspended solids can be approximated by using a continuum approach. The amount of rocks in the mixture will be described as a fraction (α_s). The rocks do not all have the same diameter but are distributed over a certain range. The total solids fraction can be divided into K sub fractions, where the total solid concentration is defined as follows:

$$\alpha_s = \sum_{k=1}^{K} \alpha_{s,k} \tag{7.1}$$

For each fraction a particular settling velocity with respect to the mixture velocity should be calculated based on the specific diameter of the particle of that fraction and the concentration of the mixture. Notice that the total volume concentration is by definition given by the following equation:

$$\alpha_f + \sum_{k=1}^{K} \alpha_{s,k} = 1 \tag{7.2}$$

Where α_f is the concentration of the fluid and $\alpha_{s,k}$ is the concentration of a solid fraction. The total mixture density ρ_m can be calculated by using equation 7.3, by assuming a constant density of the solids for each fraction.

$$\rho_m = \alpha_s \rho_s + (1 - \alpha_s)\rho_f \tag{7.3}$$

27

Conservation and momentum equation

The mixture of fluid and rocks is treated as a single fluid with density ρ_m, velocity v_m and pressure p. The mixture is assumed to be incompressible with a non-constant density [Goeree & van Rhee, 2013]. This means ρ_m is time dependent i.e. $\rho_m = \rho_m(t)$.

Continuity equation

The continuity equation for a closed fallpipe, when looking at the in and outflow of each segment, can be written by equation 7.4. An overview of one segment is given in figure 7.1. Note: The velocity is defined positive upward. The velocities during subsea rock installation are mostly in downward direction and therefore negative.

$$\frac{\partial}{\partial t} \int_V \rho_m dV + \oint_{A_1} \rho_m v_m dA_1 - \oint_{A_2} \rho_m v_m dA_2 = 0 \tag{7.4}$$

Where the first term describes the density change in time in control volume V, the second term describes the flux through boundary A_1 and the third term describes the flux through boundary A_2. Where the area $A_1 = A_2$. The continuity equation should be equal to zero if no extra mass will be added to or subtracted from the control volume (source or sink). In a closed fallpipe the inner area is constant over the length of the fallpipe and the volume of the element is the inner area multiplied with the length of the element (Δz). By dividing equation 7.4 by the volume of the element the continuity equation for a closed fallpipe can be written as follows:

$$\frac{\partial \rho_m}{\partial t} + \frac{\partial(\rho_m v_m)}{\partial z} = 0 \tag{7.5}$$
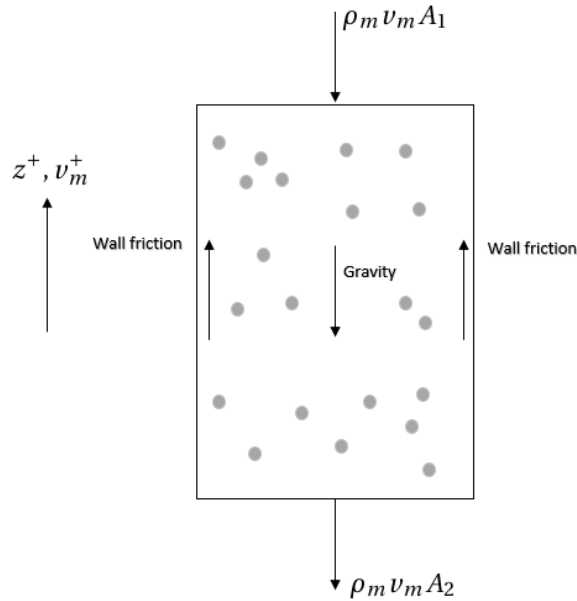
Figure 7.1: Forces acting in an element of a closed fallpipe

Momentum equation

The equation of motion of a fluid is governed by the Navier-Stokes equation. For a fallpipe the equation of motion is given by equation 7.6. An overview of the forces acting in a section for a closed fallpipe is given in figure 7.1.

$$\frac{\partial}{\partial t} \int_V \rho_m v_m dV + \oint_{A_1} \rho_m v_m^2 dA_1 - \oint_{A_2} \rho_m v_m^2 dA_2 = -\oint_{A_1} p dA_1 + \oint_{A_2} p dA_2 - \int_V |\rho_m g| dV + F_{viscous} \tag{7.6}$$

Where the first term is the change of momentum in time, the second term is the momentum flux through boundary A_1, the third terms is the momentum flux through boundary A_2, the fourth term is the pressure

term at the upper boundary, the fifth term is the pressure term at the lower boundary, the sixth term is the gravity force and the last term is the friction force due to wall friction.

Viscous stresses
The total viscous stresses for a closed fallpipe depends on the wall friction, while for a semi-closed fallpipe it is a combination of wall friction and Carnot losses. The pressure loss due to friction for a close fallpipe can be described as follows[Matoušek, 2004]:

$$\frac{dp}{dz} = \frac{4\tau_m}{D} \tag{7.7}$$

Where D is the diameter of the fallpipe. By using the Darcy-Weisbach equation, the pressure loss due to friction over a certain length (Δz) can be written as follows:

$$\Delta p_{friction} = \frac{\Delta z}{2D} \lambda_m \rho_m v_m^2 \tag{7.8}$$

The friction factor λ_m depends on the Reynolds number and relative roughness of the pipe and can be obtained from the Moody diagram in figure 7.2. The Reynolds number and the relative roughness of the pipe can be calculated by the following equations:

$$Re = \frac{v_m D \rho_m}{\mu} \tag{7.9}$$

$$RPR = \frac{\epsilon}{D} \tag{7.10}$$

Where μ is the dynamic viscosity of the medium, ϵ is the pipe roughness and $\frac{\epsilon}{D}$ is the relative pipe roughness.
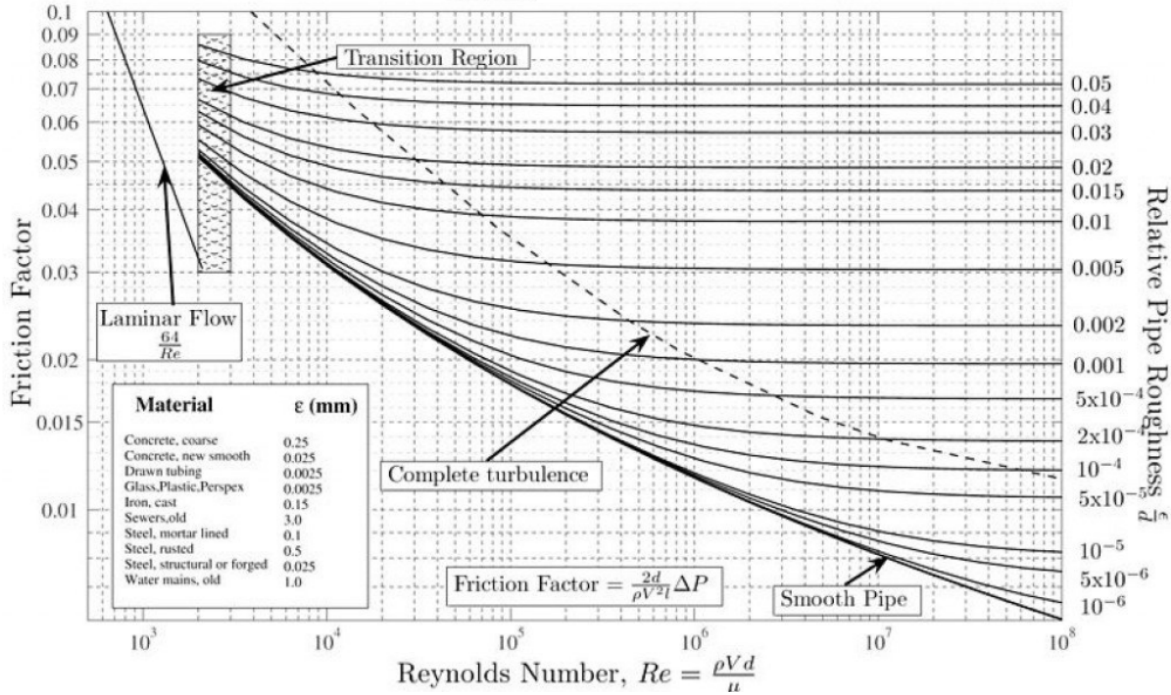
Figure 7.2: Moody diagram for determine the friction coefficient

For a closed fallpipe the pressure loss due to friction ($\Delta p_{friction}$) can be written in terms of the wall shear stress in the following way by only taken into account the friction due to the mixture:

$$\tau_m = \frac{\lambda_m}{2D} \rho_m v_m^2 \tag{7.11}$$

Implementing the viscous term equation 7.6 results in the following momentum equation for a closed fallpipe:

$$\frac{\partial}{\partial t}\int_V \rho_m v_m dV + \oint_{A_1}\rho_m v_m^2 dA_1 - \oint_{A_2}\rho_m v_m^2 dA_2 = -\oint_{A_1} p dA_1 + \oint_{A_2} p dA_2 + \frac{1}{2D}\rho_m v_m^2 \lambda_m - \int_V |\rho_m g| dV \quad (7.12)$$

Transport of concentration

Solving the continuity and momentum equation will result in a velocity and pressure field in the fallpipe. The transport of solids can be described by using the transport equation for each concentration fraction individually. When looking at the advection part and neglecting the diffusion part, the transport equation can be written as follows:

$$\frac{\partial}{\partial t}\int_V \alpha_{s,k} dV + \oint_{A_1}\alpha_{s,k} v_{fall,k} dA_1 - \oint_{A_2}\alpha_{s,k} v_{fall,k} dA_2 = 0 \quad (7.13)$$

Where the first term is the total change of concentration in time, the second term is the flow of concentration through the upper boundary and the third term is the flow of concentration through the lower boundary of the element.

7.2. COMPUTATIONAL METHOD

The drift-flux model is used to model the process of subsea rock installation. This method can be generally divided into two parts. The first part is modelling the mixture flow and the second part is the sediment transport. To model the mixture flow, the fractional step method is used. To describe the transport of sediment, the mixture velocity, settling velocity of the rocks and the advection-diffusion equation are used.

7.2.1. NUMERICAL IMPLEMENTATION

For the numerical implementation it is chosen to use a staggered grid, which means in comparison with a Cartesian grid, the variables pressure and velocity are not located at the same location. See figure 7.4[Hirsch Charles, 2007].

(a) Cartesian grid
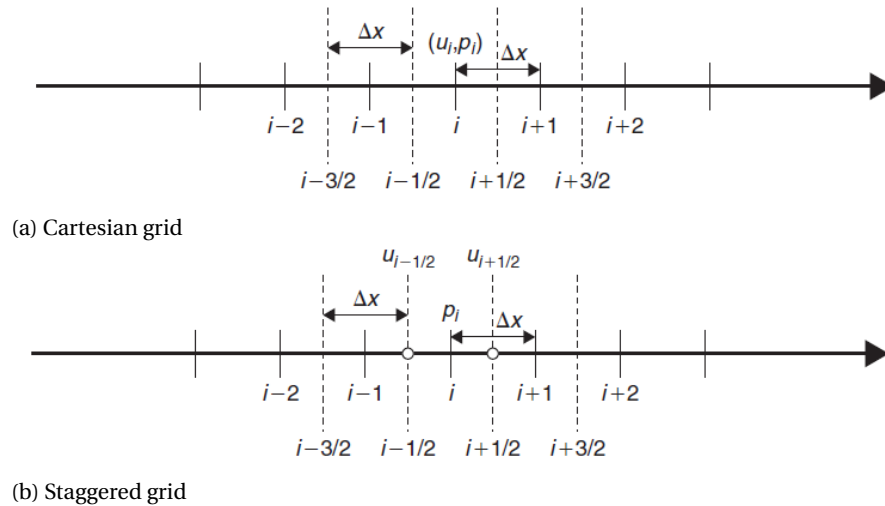
(b) Staggered grid

Figure 7.3: Cartesian grid and staggered grid

For a Cartesian grid, the velocity and pressure are located at the centre of each cell while for a staggered grid the velocity is located at the boundaries of the cell and the pressure is located at the centre of the cell. The main advantage of a staggered grid above a Cartesian grid is that the pressure and velocity is less coupled, which makes the numerical model more stable. The variables density ρ, concentration α_s and pressure p are located in the centre of the cell and only the velocity $\vec{v}$ is located at the cell boundaries. This results in two different control volumes for the mass and momentum conservation, as shown in figure 7.4.

(a) Control volume for mass conservation   (b) Control volume for momentum conservation
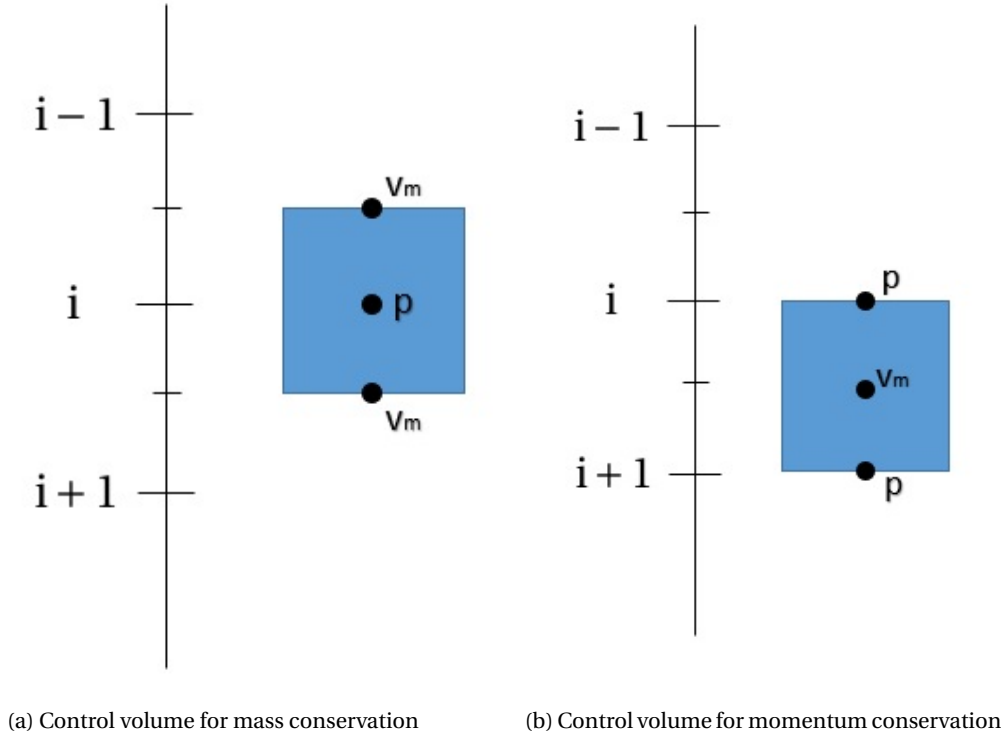
Figure 7.4: Control volume for mass and momentum conservation

7.2.2. FRACTIONAL STEP METHOD

In the fractional step method an intermediate velocity will be obtained by simply omitting the pressure term in the momentum equation,given by equation 7.12. The pressure term will be obtained by solving a Poisson equation 7.27 and finally the flow velocity can be determined by correcting the intermediate velocity for the pressure.

The total length of the fallpipe will be divided into a number of segments, which is the total length of the fallpipe divided by the length of each segment Δz. Note that for keeping the numerical scheme stable, the Courant-Friedrichs-Lewy (CFL) condition should be satisfied [Hirsch Charles, 2007]. The Courant-Friedrichs-Lewy condition is given by equation 7.14. This condition means that the time step should be small enough to ensure no element will be jumped over during a time step, which would result in numerical instability.

$$C = \frac{v\Delta t}{\Delta z} \leq 1 \tag{7.14}$$

Where v is a velocity, Δt is time step and Δz is spacial step. The input is given as a certain production in tonnes per hour and a certain settling velocity of the rocks ($\vec{v}_s$). Based on these two parameters the concentration of the mixture can be obtained, by using equation 7.15 and 7.16.

$$\rho_{m,input} = \alpha_s \rho_s + (1 - \alpha_s)\rho_{air} \tag{7.15}$$

Where ρ_{air} is the density of air. The density of air is small in comparison with the density of rock, which makes it valid to neglect the air part in the mixture density.

$$\alpha_{s,in} = \frac{P_{in}}{\vec{v}_s A \rho_s} \tag{7.16}$$

Where A is the inner area of the fallpipe. The input velocity of the rocks is equal to the settling velocity of the rocks in air over the height from the conveyor belt to the water level in the fallpipe.

The next step is to calculate the momentum at the boundaries. First an intermediate momentum ρv^* is calculated by discretization of equation 7.12 and omitting the pressure term. The equation for the three different locations, boundary(i= $\frac{1}{2}$), mid locations ($\frac{1}{2}$< i <$i_{max} + \frac{1}{2}$) and the lower boundary (i=$i_{max} + \frac{1}{2}$) are

given by equation 7.17, 7.18 and 7.19 respectively. For the momentum discretization a central difference scheme is used. Important to notice is that the same equations are valid for modelling a water flow in the fallpipe. The only difference is the input density.

For modelling a water flow the input density is equal to the density of water, $\rho_{m,input} = \rho_w$ and $\alpha_{s,in} = 0$. When the concentration solids is equal to 0, it means the mixture density ρ_m will automatically transform to the water density because of equation 7.3.

$$\rho_{m,\frac{1}{2}} v^*_{m,\frac{1}{2}} = v^t_{in} \rho^t_{m,in} \tag{7.17}$$

$$(\rho_{m,i+\frac{1}{2}} v_{i+\frac{1}{2}})^* = v^t_{m,i+\frac{1}{2}} \rho^t_{m,i+\frac{1}{2}} - \frac{\Delta t}{2\Delta z}\left((\rho_{m,i-\frac{1}{2}} v^2_{m,i-\frac{1}{2}}) - (\rho_{m,i+\frac{3}{2}} v^2_{m,i+\frac{3}{2}})\right)^t ...$$
$$+ \frac{\Delta t}{2D}\lambda(\rho_{m,i+\frac{1}{2}} v^2_{m,i+\frac{1}{2}})^t - \Delta t |\rho^t_{m,i+\frac{1}{2}} g| \tag{7.18}$$

$$\rho_{m,i_{max}+\frac{1}{2}} v^*_{m,i_{max}+\frac{1}{2}} = \rho_{m,i_{max}-\frac{1}{2}} v^*_{m,i_{max}-\frac{1}{2}} \tag{7.19}$$

When the intermediate momentum (ρv^*) is calculated for all the locations in the fallpipe, the velocity will be corrected by the pressure for the new time step, which can be calculated by solving a Poisson equation. The Poisson equation ensures that continuity is conserved. The corrected velocity is the mixture velocity for the new time step.

Upper boundary cell
Looking at the density change of the top cell ($i = 1$), as displayed in figure 7.5 an equation for the pressure can be obtained. The density change of the control volume depends on the in an outflow. The inflow at this location is set as a boundary condition namely $\rho_{m,in}$ and v_{in}. Important to notice is that z-direction and velocity is positive upwards.
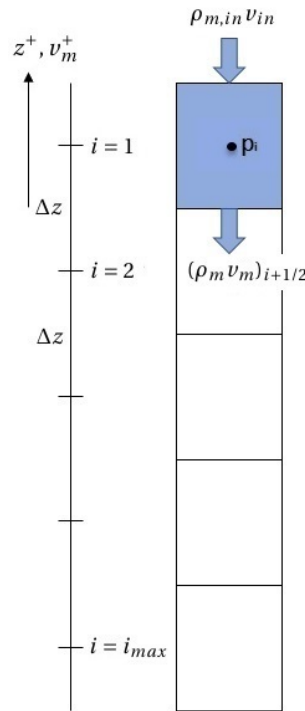

Figure 7.5: Overview of control volume for upper cell

Writing equation 7.4 in discrete form, the following equation for the density change of the control volume is obtained:

$$\Delta x \Delta z \frac{\partial \rho_{m,i}}{\partial t} = \Delta x \left(\rho_m v_m \right)_{i+\frac{1}{2}}^{t+1} - \Delta x \left(\rho_{m,in} v_{in} \right) \tag{7.20}$$

Where v_m^{t+1} is the mixture velocity at the new time step and Δx is the width of the element. Because each term is multiplied with Δx, the equation can be divided by Δx. The intermediate velocity is calculated by using the momentum equation and omitting the pressure term. The velocity for the new time step can be calculated by including the pressure term, given by the following equation:

$$\rho_{m,i+\frac{1}{2}} \int_V \frac{v_{m,i+\frac{1}{2}}{}^{t+1} - v_{i+\frac{1}{2}}^*}{\Delta t} dV = - \oint_{A_1} p\, dA_1 + \oint_{A_2} p\, dA_2 \tag{7.21}$$

Where area $A_1 = A_2$ and volume (V) is equal to the area multiplied with Δz. The velocity and pressure are not located at the same location because of the staggered grid. Looking at the control volume in figure 7.4 and dividing the equation by the volume of the element, an expression for the velocity for the new time step is obtained based on the intermediate velocity and pressure.

$$\rho_{m,i+\frac{1}{2}} v_{m,i+\frac{1}{2}}^{t+1} = \rho_{m,i+\frac{1}{2}} v_{m,i+\frac{1}{2}}^* + \frac{\Delta t}{\Delta z} \left(p_{i+1}^{t+1} - p_i^{t+1} \right) \tag{7.22}$$

Substitution of equation 7.22 into equation 7.20, the following equation is obtained:

$$\Delta z \frac{\partial \rho_{m,i}}{\partial t} = (\rho_m v_{m,i+\frac{1}{2}}^*) + \frac{\Delta t}{\Delta z} \left(p_{i+1}^{t+1} - p_i^{t+1} \right) - \rho_{m,in}^t v_{in}^t \tag{7.23}$$

Rearranging the pressure terms to the left hand side results in the Poisson equation for location i=1, shown in the following equation. Important to notice is that the inlet velocity of the rock mixture has an effect on the pressures in the fallpipe.

$$\frac{p_{i+1}^{t+1} - p_i^{t+1}}{\Delta z^2} = \frac{1}{\Delta t} \frac{\rho_m^t - \rho_m^{t-1}}{\Delta t} + \frac{1}{\Delta z \Delta t} \left(\rho_{m,in}^t v_{in}^t - \rho_m v_{m,i+\frac{1}{2}}^* \right) \tag{7.24}$$

Mid cell

The Poisson equation for location $1 < i < i_{max}$, which are all the cells of the fallpipe except the cells at the boundaries. An example for a specific control volume is given in figure 7.6. The flow into the control volume is given by $(\rho_m v)_{i-\frac{1}{2}}$ and the flow out of the control volume is $(\rho_m v)_{i+\frac{1}{2}}$.
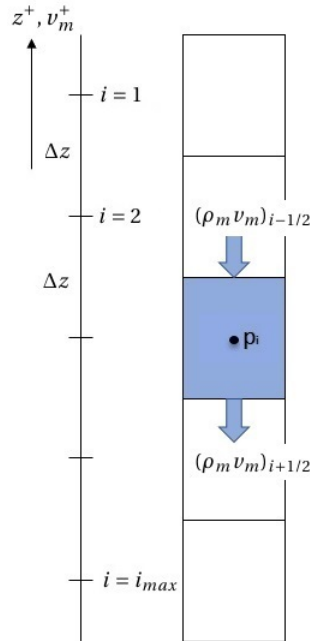
Figure 7.6: Overview of control volume for a cell in the middle

The density change in the control volume can be described by the following equation:

$$\Delta z \frac{\partial \rho_{m,i}}{\partial t} = \left(\rho_m v_m \right)^{t+1}_{i+\frac{1}{2}} - \left(\rho_m v_m \right)^{t+1}_{i-\frac{1}{2}} \tag{7.25}$$

Substitution of equation 7.22 into equation 7.25, the following equation for the continuity is obtained.

$$\Delta z \frac{\partial \rho_{m,i}}{\partial t} = \left(\rho_m v^*_{m,i+\frac{1}{2}} + \frac{\Delta t}{\Delta z} (p^{t+1}_{i+1} - p^{t+1}_i) \right) - \left(\rho_m v^*_{m,i-\frac{1}{2}} + \frac{\Delta t}{\Delta z} (p^{t+1}_i - p^{t+1}_{i-1}) \right) \tag{7.26}$$

Rearranging of the pressure terms and discretization of the density change over time term leads to the Poisson equation for the cells in the middle. Given by the following equation:

$$\frac{p^{t+1}_{i+1} - 2p^{t+1}_i + p^{t+1}_{i-1}}{\Delta z^2} = \frac{1}{\Delta t} \frac{\rho^t_m - \rho^{t-1}_m}{\Delta t} + \frac{1}{\Delta z \Delta t} \left(\rho_m v^*_{m,i-\frac{1}{2}} - \rho_m v^*_{m,i+\frac{1}{2}} \right) \tag{7.27}$$

Lower boundary cell
At the lower boundary cell, the boundary condition for the pressure at location i_{max+1} is equal to the surrounding hydrostatic pressure, as shown in figure 7.7.
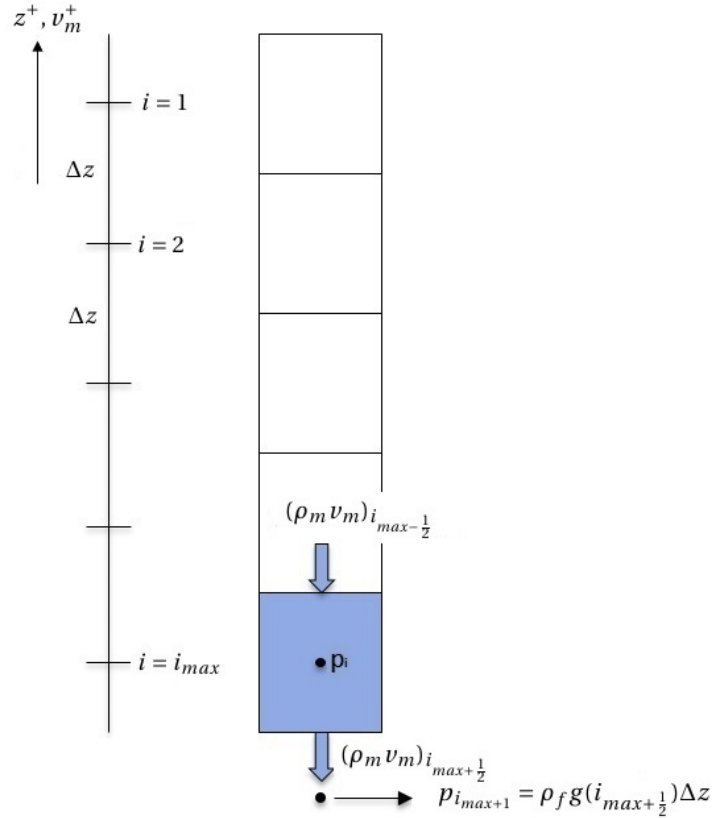
Figure 7.7: Overview of control volume for the last cell

The hydrostatic pressure at that location can be calculated as follows:

$$p_{i_{max+1}} = \rho_f g z_{i_{max+1}} \tag{7.28}$$

Where $z_{i_{max+1}}$ is the depth of location i_{max+1}. Equation 7.28 can be written in terms of Δz as follows:

$$p_{i_{max+1}} = \rho_f g i_{max+\frac{1}{2}} \Delta z \tag{7.29}$$

Substitution of equation 7.29 into equation 7.26 and by using equation 7.19, the Poisson equation can be obtained for the lower boundary cell. Given as follows:

$$\frac{p_{i-1}^{t+1} - 2p_{i_{max}}^{t+1} + p_{i_{max+1}}^{t+1}}{\Delta z^2} = \frac{1}{\Delta t}\frac{\rho_m^t - \rho_m^{t-1}}{\Delta t} \tag{7.30}$$

The equation can be rewritten by using equation 7.29 into the following equation:

$$\frac{p_{i-1}^{t+1} - 2p_{i_{max}}^{t+1}}{\Delta z^2} = \frac{1}{\Delta t}\frac{\rho_m^t - \rho_m^{t-1}}{\Delta t} - \frac{\rho_f g i_{max+\frac{1}{2}}}{\Delta z} \tag{7.31}$$

Pressure term and new velocity

For solving the pressure at each location the inverse matrix method is used. This way the pressure will be calculated for each location simultaneously but it can also be solved by using an iteration process e.g. Gauss-Seidel iteration [Hirsch Charles, 2007]. The pressure can be calculated in the following way:

$$A \cdot p = Q \tag{7.32}$$

$$\frac{1}{\Delta z^2}\begin{pmatrix} -1 & 1 & 0 & 0 & 0 & 0 \\ 1 & -2 & \ddots & 0 & 0 & 0 \\ 0 & \ddots & \ddots & \ddots & 0 & 0 \\ 0 & 0 & \ddots & \ddots & \ddots & 0 \\ 0 & 0 & 0 & \ddots & -2 & 1 \\ 0 & 0 & 0 & 0 & 1 & -2 \end{pmatrix}\begin{pmatrix} p_1^{t+1} \\ \vdots \\ \vdots \\ p_i^{t+1} \\ \vdots \\ p_{i_{max}}^{t+1} \end{pmatrix} = \begin{pmatrix} \frac{1}{\Delta t^2}\left(\rho_m^t - \rho_m^{t-1}\right) + \frac{1}{\Delta z \Delta t}\left(\rho_{m,in}^t v_{in}^t - \rho_m v_{m,i+\frac{1}{2}}^*\right) \\ \vdots \\ \vdots \\ \frac{1}{\Delta t^2}\left(\rho_m^t - \rho_m^{t-1}\right) + \frac{1}{\Delta z \Delta t}\left(\rho_m v_{m,i-\frac{1}{2}}^* - \rho_m v_{m,i+\frac{1}{2}}^*\right) \\ \vdots \\ \frac{1}{\Delta t}\left(\rho_m^t - \rho_m^{t-1}\right) - \frac{\rho_f g(i_{max+\frac{1}{2}})}{\Delta z} \end{pmatrix} \tag{7.33}$$

Where p is the pressure vector with length i_{max}, A is an i_{max} x i_{max} matrix and Q is a vector with length i_{max} which can be obtained by calculating the right hand side of equation 7.24, 7.27 and 7.31 by using the intermediate velocity for each location. When the pressure at each location is known and the intermediate velocity is calculated, the velocity for the new time step can be calculated by the following equation:

$$v_{m,i+1/2}^{t+1} = \frac{\rho_{m,i+1/2}^t v_{i+1/2}^*}{\rho_{m,i+1/2}^t} + \frac{\Delta t}{\Delta z \rho_{m,i+1/2}^t}(p_{i+1}^{t+1} - p_i^{t+1}) \tag{7.34}$$

7.2.3. FALL VELOCITY

The total input of rock is divided into a number of fractions (K) and for each fraction the total fall velocity should be calculated. Following Goeree, Keetels and others the total fall velocity of the solids is a combination of the mixture velocity and the relative velocity between the solids and the mixture [Goeree *et al.*, 2016]. Given by the following equation:

$$v_{fall,k} = v_m + w_{sm,k} \tag{7.35}$$

Where $v_{fall,k}$ is the total fall velocity of the solids fraction and $w_{sm,k}$ is the relative velocity between the solids and the mixture. The relative velocity between the solids and the mixture can be calculated by using the following equation:

$$w_{sm,k} = w_{r,k} - \frac{\rho_s}{\rho_m}\sum_{k=1}^{K}(\alpha_{s,k}w_{r,k}) \tag{7.36}$$

Where $w_{r,k}$ is the relative velocity with respect to the liquid phase. Mirza and Richardson gave a relation to determine the relative velocity with respect to the liquid phase based on the terminal settling velocity of a particle in quiescent fluid. The relation is given as follows:

$$w_{r,k} = w_{e,p}\left(1 - \sum_{k=1}^{K}\alpha_{s,k}\right)^{n_k-1} \tag{7.37}$$

Where $w_{e,p}$ is the terminal settling velocity of a particle in quiescent fluid, corrected for the fallpipe influence and n_k is the Richardson and Zaki index for each fraction given by equation 3.13. The terminal settling velocity (w_e) for a particle is determined following Ferguson and Church and is given by equation 3.10. To correct the velocity for the fallpipe influence, the equation of Newton is used [Li *et al.*, 2014]:

$$w_{e,p} = w_e \left(1 - \left(\frac{d}{D}\right)^2\right) \sqrt{\left(1 - 0.5\left(\frac{d}{D}\right)\right)} \qquad (7.38)$$

Where d is the particle diameter and D is the diameter of the fallpipe. Looking at equation 7.38, it can be concluded that, if the diameter of the rock increases, the settling velocity decreases. The fallpipe will have less influence on smaller particle diameters. During subsea rock installation larger particle diameters are used, meaning that the influence of the fallpipe should be taken into account.

7.2.4. TRANSPORT OF SOLIDS

The total input of rock is divided into a number of fractions. Each fraction has its own settling velocity and so its own total fall velocity. The transport of solids can be described by looking at the concentration change in time due to in and outflow of concentration. For a closed fallpipe an overview is given in figure 7.8. Important to notice is that for stability reasons an upwind discretization scheme is used. The upwind scheme assumes that the outflow flux will be calculated at location i instead of location $i + \frac{1}{2}$. Note that by implementing an upwind scheme the transport of solids can only be described in downward direction.
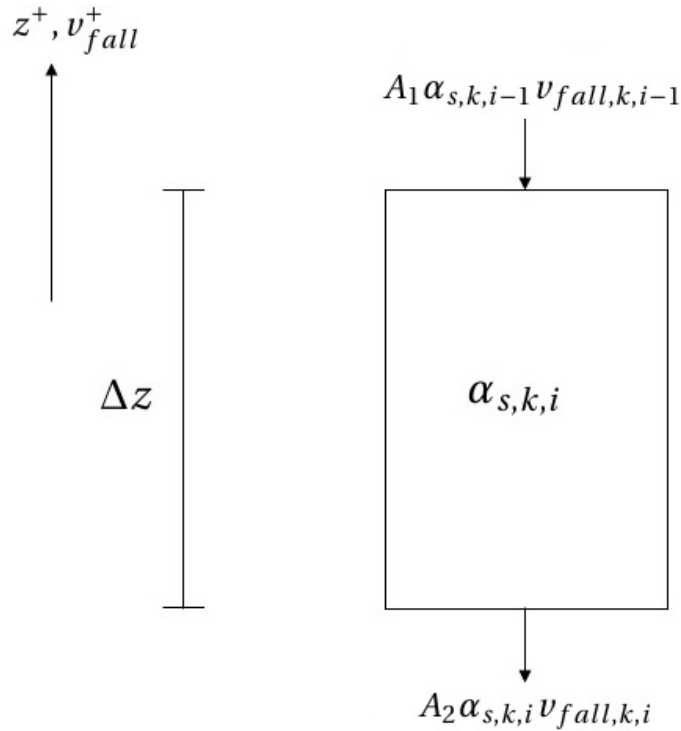
Figure 7.8: Concentration balance over a closed element

The concentration change in the element over time can be described in integral form as follows:

$$\frac{\partial}{\partial t} \int_V \alpha_{s,k} dV + \oint_{A_1} v_{fall,k} \alpha_{s,k} dA_1 - \oint_{A_2} v_{fall,k} \alpha_{s,k} dA_2 = 0 \qquad (7.39)$$

Where V can be written as the area of the pipe ($A_1 = A_2$) multiplied with the height of the element (Δz). Writing equation 7.39 in discrete form and by dividing by the volume, the following equation for the solids transport can be obtained:

$$\alpha_{s,k,i}^{t+1} = \alpha_{s,k,i}^t + \frac{\Delta t}{\Delta z}\left(\alpha_{s,k,i}^t v_{fall,k,i}^{t+1} - \alpha_{s,k,i-1}^t v_{fall,k,i-1}^{t+1}\right) \tag{7.40}$$

This equation is only valid for a closed fallpipe where the diameter of the pipe is constant over the length. The total concentration at each cell can be determined by the summation of the concentration of each fraction in a cell. If the total concentration and the velocity in each cell is determined, the production in kilogram per second can be calculated by the following equation:

$$P_{i+\frac{1}{2}} = A_{i+\frac{1}{2}} \rho_s v_{fall,i+\frac{1}{2}}^{t+1} \alpha_{s,i+\frac{1}{2}}^{t+1} \tag{7.41}$$

Before moving to the next time step the density of the mixture in the element should be updated depending on the concentration for the new time step. The new mixture density is defined as follows:

$$\rho_m^{t+1} = \alpha_s^{t+1}\rho_s + (1 - \alpha_s^{t+1})\rho_w \tag{7.42}$$

The new obtained density at each cell is used in the continuity and momentum equation to obtain the pressure term for the new time step. This process continues till the simulation time ends.

7.3. CLOSED FALLPIPE WITH WATER INLET SECTION

In reality the closed fallpipe has an in and outflow possibility for water as well. To model the in and outflow, a mass source and a momentum source are implemented in respectively the continuity and momentum equation. A schematic overview is given in figure 7.9.
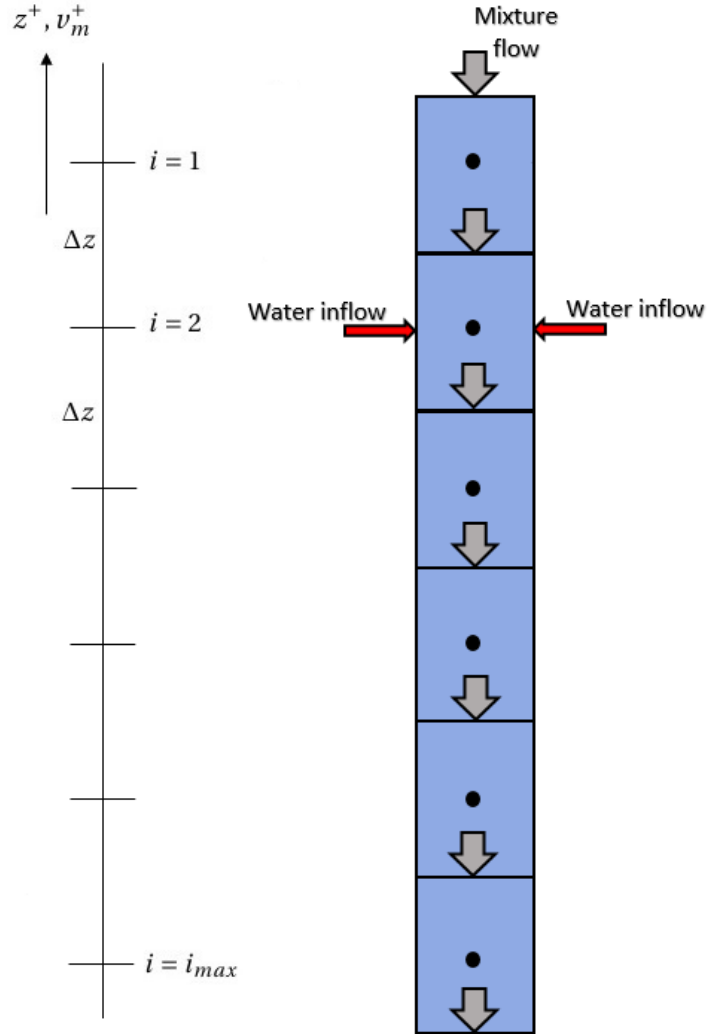
Figure 7.9: Overview of a fallpipe with a water inlet at the top

7.3.1. CONTINUITY AND MOMENTUM EQUATION

When looking at the element with an inlet section, shown in figure 7.10, the continuity equation can be conducted. For the other elements equation 7.4 is still valid. The continuity equation for the open element is given as follows:

$$\frac{\partial}{\partial t} \int_V \rho_m dV + \oint_{S_1} \rho_m v_m dS_1 - \oint_{S_2} \rho_m v_m dS_2 - 2\oint_{S_3} \rho_f v_{flow} dS_3 = 0 \tag{7.43}$$

Where S_1 is the top surface of the element for the mixture flow(Δx), S_2 is the bottom surface of the element for the mixture flow(Δx), S_3 is the surface of the inflow area ($\Delta z \mu_{area}$) and v_{flow} is the flow velocity in or out of the element. Writing the in and outflow of mass in explicit form over the element equation 7.44 is obtained. Important to notice is that the velocity is positive upward.

$$\Delta x \Delta z \frac{\rho_{m,i}^{t+1} - \rho_{m,i}^t}{\Delta t} = \Delta x (\rho_m v_m)_{i+\frac{1}{2}}^{t+1} - \Delta x (\rho_m v_m)_{i-\frac{1}{2}}^{t+1} + 2\rho_f v_{flow,i}^{t+1} \mu_{area} \Delta z \tag{7.44}$$

Where Δx is the in and outflow area of the mixture and μ_{area} is a fraction of Δz which is open for water inflow or outflow. The equation can be rewritten to the continuity equation for the open element.

$$\frac{\rho_{m,i}^{t+1} - \rho_{m,i}^{t}}{\Delta t} = \frac{(\rho_m v_m)_{i+\frac{1}{2}}^{t+1} - (\rho_m v_m)_{i-\frac{1}{2}}^{t+1}}{\Delta z} + \frac{2\rho_f v_{flow,i}^{t+1}\mu_{area}}{\Delta x} \tag{7.45}$$

Where the term at the right hand side is the in or outflow term, depending on the flow velocity, the density of the fluid flowing in and the area factor(μ_{area}). The flow velocity depends on the difference of the pressure inside the fallpipe and outside the fallpipe and is calculated by equation 7.51. If v_{flow} is positive, water will start flowing into the element and if v_{flow} is negative, water will flow out of the element.
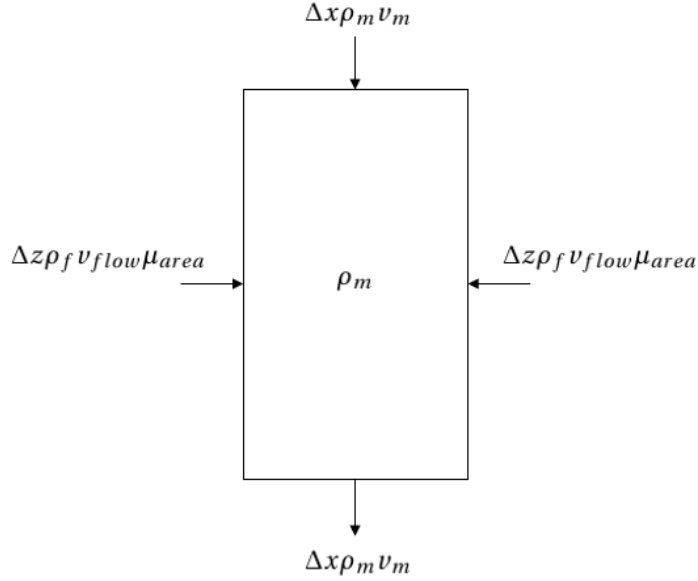
Figure 7.10: Overview of an open segment

For calculating the pressure in the fallpipe the fractional step method is used. Which is explained in more detail in paragraph 7.2.1. Substitution of equation 7.22 into equation 7.45 results in the following expression for the continuity equation for an open section:

$$\frac{\rho_{m,i}^{t+1} - \rho_{m,i}^{t}}{\Delta t} = \frac{(\rho_m v_{m,i+\frac{1}{2}}^{*}) + \frac{\Delta t}{\Delta z}\left(p_{i+1}^{t+1} - p_{i}^{t+1}\right) - (\rho_m v_{m,i-\frac{1}{2}}^{*}) + \frac{\Delta t}{\Delta z}\left(p_{i}^{t+1} - p_{i-1}^{t+1}\right)}{\Delta z} + \frac{2\rho_f v_{flow,i}^{t+1}\mu_{area}}{\Delta x} \tag{7.46}$$

Rearranging the pressure components results in the pressure equation for the open element. Important to notice is that the density change is one time step behind. The assumption is made that the density change of the previous time step is equal to the density change for the new time step.

$$\frac{p_{i+1}^{t+1} - 2p_{i}^{t+1} + p_{i-1}^{t+1}}{\Delta z^2} = \frac{\rho_m^t - \rho_m^{t-1}}{\Delta t^2} - \frac{\left(\rho_m v_{m,i+\frac{1}{2}}^{*}\right) - \left(\rho_m v_{m,i-\frac{1}{2}}^{*}\right)}{\Delta t \Delta z} - \frac{2\rho_f v_{flow}^{t+1}\mu_{area}}{\Delta x \Delta t} \tag{7.47}$$

Where the inlet will only be applied in the second element, the pressure equation for the other locations are equal to equation 7.24 for the upper cell, equation 7.27 for the other cell in the middle and equation 7.31 for the last cell. Combining these equations results in the following matrix for calculating the pressure.

$$\frac{1}{\Delta z^2}\begin{pmatrix} -1 & 1 & 0 & 0 & 0 & 0 \\ 1 & -2 & \ddots & 0 & 0 & 0 \\ 0 & \ddots & \ddots & \ddots & 0 & 0 \\ 0 & 0 & \ddots & \ddots & \ddots & 0 \\ 0 & 0 & 0 & \ddots & -2 & 1 \\ 0 & 0 & 0 & 0 & 1 & -3 \end{pmatrix}\begin{pmatrix} p_1^{t+1} \\ \vdots \\ \vdots \\ p_i^{t+1} \\ \vdots \\ p_{i_{max}}^{t+1} \end{pmatrix} = \begin{pmatrix} \frac{\rho_m^t - \rho_m^{t-1}}{\Delta t^2} + \frac{\rho_{m,in}^t v_{in}^t - (\rho_m v_{m,\frac{3}{2}}^*)}{\Delta t \Delta z} \\ \frac{1}{\Delta t^2}\left(\rho_m^t - \rho_m^{t-1}\right) + \frac{1}{\Delta z \Delta t}\left(\rho_m v_{m,\frac{3}{2}}^* - \rho_m v_{m,\frac{5}{2}}^*\right) - \frac{2}{\Delta x \Delta t}(\mu_{area}\rho_f v_{flow}^{t+1}) \\ \vdots \\ \frac{1}{\Delta t^2}\left(\rho_m^t - \rho_m^{t-1}\right) + \frac{1}{\Delta z \Delta t}\left(\rho_m v_{m,i-\frac{1}{2}}^* - \rho_m v_{m,i+\frac{1}{2}}^*\right) \\ \vdots \\ \frac{1}{\Delta t}\left(\rho_m^t - \rho_m^{t-1}\right) - \frac{\rho_m g i_{max+\frac{1}{2}}}{\Delta z} \end{pmatrix}$$

$$(7.48)$$

The introduction of the inflow does not only change the pressure distribution, it will also change te momentum. To enforce momentum conservation the inflow is incorporated by the following way:

$$\frac{\partial}{\partial t}\int_V \rho_m v_m dV + \oint_{S_1}\rho_m v_m^2 dS_1 - \oint_{S_2}\rho_m v_m^2 dS_2 + \underbrace{\oint_{S_3}\rho_f v_{flow}^2 dS_3}_{\text{Momentum source term}} = -\oint_{S_1}p dS_1 + \oint_{S_2}p dS_2 ...$$

$$-\int_V |\rho_m g| dV + \frac{1}{2D}\rho_m v_m^2 \lambda_m \quad (7.49)$$

Where the momentum source term is positive when water flows in and is negative when water flows out of the element. Writing equation 7.49 in discrete form results in the following equation:

$$(\rho_{m,i+\frac{1}{2}}v_{i+\frac{1}{2}})^* = v_{m,i+\frac{1}{2}}^t \rho_{m,i+\frac{1}{2}}^t - \frac{\Delta t}{2\Delta z}\left(\rho_{m,i-\frac{1}{2}}v_{m,i-\frac{1}{2}}^2 - \rho_{m,i+\frac{3}{2}}v_{m,i+\frac{3}{2}}^2\right)^t ...$$

$$-\frac{2\Delta t}{\Delta x}\left(\rho_f v_{flow,i}^2 \mu_{area}\right)^t + \frac{\Delta t}{2D}\lambda(\rho_{m,i+\frac{1}{2}}v_{m,i+\frac{1}{2}}^2)^t - \Delta t|\rho_{m,i+\frac{1}{2}}^t g| \quad (7.50)$$

Where Δx is equal to the pipe diameter. Equation 7.50 is only valid for a element with in or outflow possibility. For all other elements equation 7.17, 7.18 or 7.19 should be used.

7.3.2. Bernoulli's equation to determine flow velocities
The pressure difference between in and outside of the fallpipe results in an in or outflow of water at the inlet section. The flow velocity is calculated by using Bernoulli's equation:

$$v_{flow} = \sqrt{\frac{2\Delta p}{\rho_f}} \quad (7.51)$$

Where Δp is the pressure difference between in and outside of the fallpipe. First an intermediate pressure (p^*) is obtained by using equation 7.48, while neglecting the inflow part i.e. v_{flow} is set to be 0. Important to say is that by using the drift-flux model a negative pressure can be calculated. This negative pressure means that there is no water in the fallpipe. When the pressure becomes smaller than 0 Pa. The pressure is forced to be 0 Pa. The pressure difference is the difference between the intermediate pressure and the hydrostatic pressure, defined as follows:

$$\Delta p = p^* - \rho_w g z_i \quad (7.52)$$

To model this in a numerical model, under-relaxation and an iteration scheme should be used. Under-relaxation decreases the possibility of divergence or oscillations in the solutions. The iteration ensures that a convergence solution for the flow velocity is obtained. When the flow velocity is determined the pressure for the new time step can be calculated by using equation 7.48. If the new pressure is calculated the mixture velocity for the new time step can be calculated by equation 7.22. The concentration development can be described in the same manner as discussed in paragraph 7.2.3 and 7.2.4.

7.4. SEMI-CLOSED FALLPIPE MODEL

The semi-closed fallpipe system used by Van Oord is built up from open-ended buckets. This means in comparison with a closed fallpipe, there is a possibility of water in- and outflow at each segment. A schematic overview of the total fallpipe is given in figure 7.11. Next to the in and outflow possibility at each segment, the bucket system has an extra pressure loss term as well, namely the Carnot losses. The Carnot losses can be calculated by using equation **??** and should be implemented into the momentum equation. Another difference is that the diameter of the bucket is not constant in z-direction.
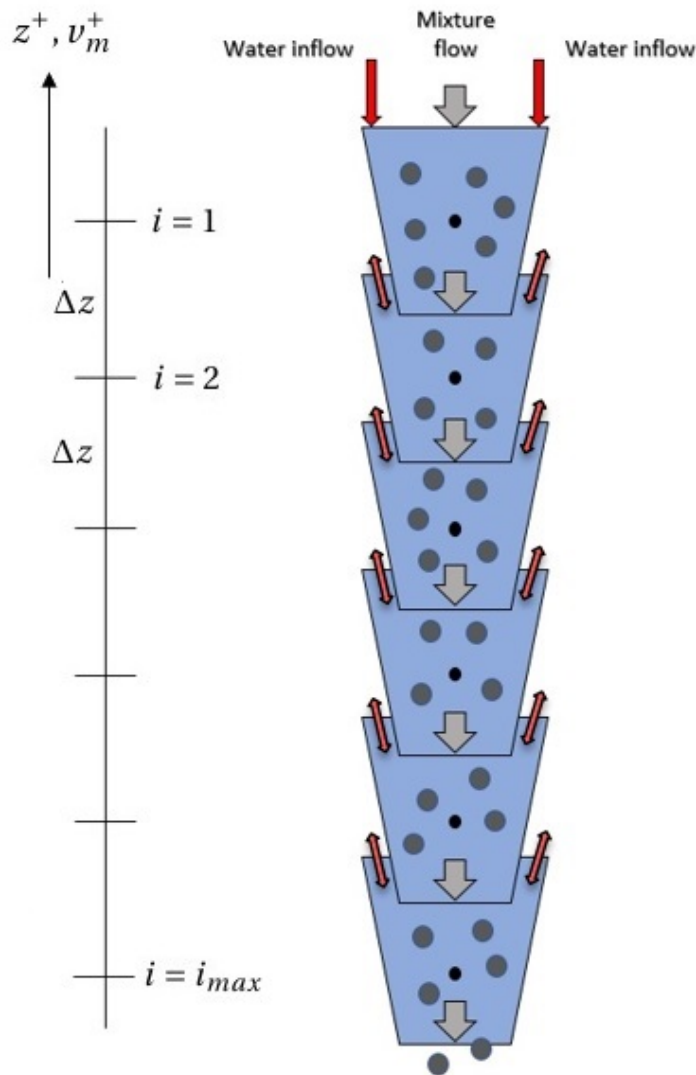
Figure 7.11: Overview of a semi-closed fallpipe

To model the in and outflow possibility in the element it is chosen to look at each bucket as a single element, shown in figure 7.12. The complete control volume will be enclosed by ABCD. While BC and EF displays respectively the control surface A_1 and A_2 for the mixture flow and surfaces AF and DE displays the in and outflow surface A_3 of the element. The areas A_1, A_2 and A_3 are shown in figure 7.13. Note that area A_1 is equal to area A_2.
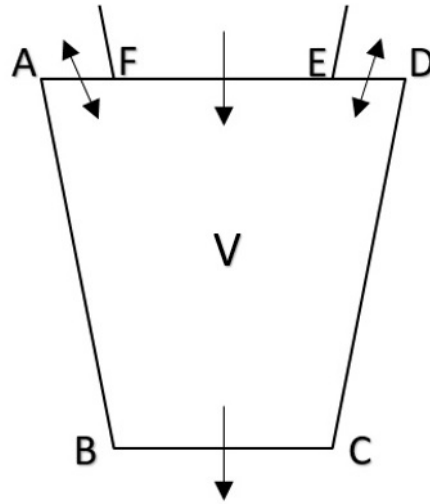
Figure 7.12: Mass control volume of a bucket
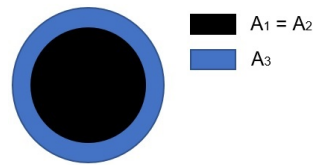
Figure 7.13: Topview of buckets showing different flow areas
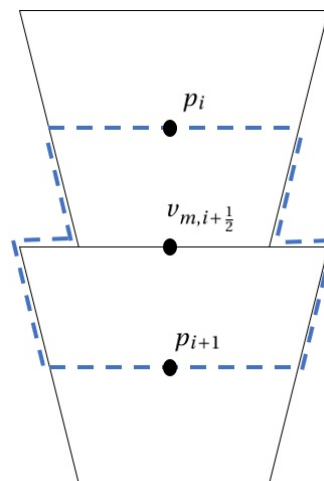
Figure 7.14: Control volume of velocity for a bucket

7.4.1. CONTINUITY AND MOMENTUM EQUATION

The continuity equation of the control volume is given in integral form as follows:

$$\underbrace{\frac{\partial}{\partial t}\int_V \rho_m dV}_{\text{Density change in time}} + \underbrace{\oint_{A_1} \rho_m v_m dA_1}_{\text{Mass inflow}} - \underbrace{\oint_{A_2} \rho_m v_m dA_2}_{\text{Mass outflow}} - \underbrace{\oint_{A_3} \rho_f v_{flow} dA_3}_{\text{Mass in or outflow due to pressure}} = 0 \qquad (7.53)$$

Where the first term describes the total density change in the control volume V, the second term describes the mass flux through boundary A_1 of the control volume, the third term describes the mass flux through boundary A_2 of the control volume and the last term is a mass source depending on flow in or out of the element. Where v_{flow} is the velocity of the in or out flow and A_3 is the flow area. Important to notice is that $A_1 = A_2$. For the following equations A_2 is replaced for A_1. The continuity equation can be written in discrete form in the following way:

$$\frac{\rho_{m,i}^{t+1} - \rho_{m,i}^{t}}{\Delta t} V = A_1 (\rho_m v_m)_{i+\frac{1}{2}}^{t+1} - A_1 (\rho_m v_m)_{i-\frac{1}{2}}^{t+1} + A_3 \rho_f v_{flow,i}^{t+1} \tag{7.54}$$

By dividing equation 7.54 by the volume of the element, the following equation can be obtained:

$$\frac{\rho_{m,i}^{t+1} - \rho_{m,i}^{t}}{\Delta t} = \frac{A_1}{V} (\rho_m v_m)_{i+\frac{1}{2}}^{t+1} - \frac{A_1}{V} (\rho_m v_m)_{i-\frac{1}{2}}^{t+1} + \frac{A_3}{V} \rho_f v_{flow,i}^{t+1} \tag{7.55}$$

The mixture velocity for the new time step can be written as an intermediate velocity and a pressure term. When looking at the control volume of the velocity, given in figure 7.14 and by using the following equation

$$\rho_{m,i+\frac{1}{2}} \int_V \frac{v_{m,i+\frac{1}{2}}^{t+1} - v_{i+\frac{1}{2}}^{*}}{\Delta t} dV = -\oint_{A_{mean,1}} p^{t+1} dA_{mean,1} + \oint_{A_{mean,2}} p^{t+1} dA_{mean,2}, \tag{7.56}$$

where $A_{mean,1}$ and $A_{mean,2}$ are respectively the upper and lower area of the control volume and are equal to each other, an equation for the mixture velocity and pressure can be obtained. Given as follows:

$$\rho_{m,i+\frac{1}{2}}^{t} v_{m,i+\frac{1}{2}}^{t+1} = \rho_{m,i+\frac{1}{2}}^{t} v_{i+\frac{1}{2}}^{*} + \frac{\Delta t}{\Delta z} (p_{i+1}^{t+1} - p_i^{t+1}) \tag{7.57}$$

Writing equation 7.57 explicit for the new mixture velocity, results in the following equation:

$$v_{m,i+\frac{1}{2}}^{t+1} = v_{i+\frac{1}{2}}^{*} + \frac{\Delta t}{\rho_{m,i+\frac{1}{2}}^{t} \Delta z} (p_{i+1}^{t+1} - p_i^{t+1}) \tag{7.58}$$

To obtain an expression for the pressure equation 7.58 should be implemented into equation 7.55. Where the volume of the element (V) is equal to mean area of the element (A_{mean}) multiplied with the length of the element (Δz).

$$\frac{\rho_m^{t+1} - \rho_m^{t}}{\Delta t} = \frac{A_1}{A_{mean} \Delta z} \left(\left((\rho_m v_m^*)_{i+\frac{1}{2}} + \frac{\Delta t}{\Delta z} (p_{i+1}^{t+1} - p_i^{t+1}) \right) - \left((\rho_m v_m^*)_{i-\frac{1}{2}} + \frac{\Delta t}{\Delta z} (p_i^{t+1} - p_{i-1}^{t+1}) \right) \right) \cdots$$
$$+ \frac{A_3}{A_{mean} \Delta z} (\rho_f v_{flow}^{t+1}) \tag{7.59}$$

Rearranging the pressure terms results in the following equation for the elements which are not located at the upper or lower boundary.

$$\frac{p_{i+1}^{t+1} - 2p_i^{t+1} + p_{i-1}^{t+1}}{\Delta z^2} = \frac{A_{mean}(\rho_m^{t} - \rho_m^{t-1})}{A_1 \Delta t^2} + \frac{1}{\Delta t \Delta z} \left((\rho_m v_m^*)_{i-\frac{1}{2}} - (\rho_m v_m^*)_{i+\frac{1}{2}} \right) - \frac{A_3}{A_1 \Delta t \Delta z} (\rho_f v_{flow,i}^{t+1}) \tag{7.60}$$

The pressure equation for the upper and lower boundary cells can be calculated following the same proceeder as described in paragraph 7.2.2, implementing the in and outflow possibility, as discussed above and taken into account the in and outflow areas of the bucket.

The momentum equation for this element can be described in integral form by including the Carnot losses as follows:

$$\underbrace{\frac{\partial}{\partial t} \int_V \rho_m v_m dV}_{\text{Change of momentum}} + \underbrace{\oint_{A_1} \rho_m v_m^2 dA_1}_{\text{Momentum flux of mixture flow}} - \underbrace{\oint_{A_2} \rho_m v_m^2 dA_2}_{\text{Momentum flux of mixture flow}} + \underbrace{\oint_{A_3} \rho_f v_{flow}^2 dA_3}_{\text{Momentum flux because of water in/outlet}} = \cdots$$
$$- \underbrace{\oint_{A_1} p dA_1}_{\text{Pressure term}} + \underbrace{\oint_{A_2} p dA_2}_{\text{Pressure term}} - \underbrace{\int_V |\rho_m g| dV}_{\text{Gravity term}} + \underbrace{F_{Carnot}}_{\text{Carnot force}} + \underbrace{F_{viscous}}_{\text{Friction force}} \tag{7.61}$$

Where the momentum flux because of water in or outlet should be negative for water inlet and positive for water outlet. The external forces, F_{Carnot} and $F_{viscous}$ can be calculated by using the following two equations:

$$F_{Carnot} = \frac{1}{2}\rho_m v_m^2 \zeta_{Carnot} = \frac{1}{2}\rho_m v_m^2 \left(1 - \frac{A_1}{A_{touch}}\right)^2 \tag{7.62}$$

$$F_{viscous} = \frac{1}{2D}\lambda\rho_m v_m^2 \tag{7.63}$$

For solving the momentum equation the fractional step method is used. By using the fractional step method first an intermediate velocity will be calculated by using equation 7.61 and omitting the pressure term. The next step is to calculate the pressure term by using the intermediate velocity. The last step is to correct the intermediate velocity for the pressure term.

To calculate the intermediate velocity for the three different locations $i = \frac{1}{2}$, $\frac{1}{2} < i < i_{max} - \frac{1}{2}$ and $i = i_{max} + \frac{1}{2}$, equations 7.64, 7.65 and 7.66 are used. Important to notice is that a staggered grid is used which means the pressure is located in the middle of the element, where the velocity is located at the boundaries of the element.

$$\rho_{m,\frac{1}{2}} v^*_{m,\frac{1}{2}} = \rho^t_{m,in} v^t_{in} \tag{7.64}$$

$$(\rho_{m,i+\frac{1}{2}} v_{i+\frac{1}{2}})^* = v^t_{m,i+\frac{1}{2}}\rho^t_{m,i+\frac{1}{2}} - \frac{A_1\Delta t}{V}\left((\rho_{m,i-\frac{1}{2}} v^2_{m,i-\frac{1}{2}})^t - (\rho_{m,i+\frac{1}{2}} v^2_{m,i+\frac{1}{2}})^t\right) - \frac{A_3\Delta t}{V}(\rho_f v^2_{flow,i})^t\,...$$
$$+ \Delta t\left(\frac{\lambda}{2D} + \zeta_{Carnot}\right)\rho^t_{m,i+\frac{1}{2}} v^2_{m,i+\frac{1}{2}} - \Delta t|\rho^t_{m,i+\frac{1}{2}}g| \tag{7.65}$$

$$\rho_{m,i_{max}+\frac{1}{2}} v^*_{i_{max}+\frac{1}{2}} = \rho_{m,i_{max}-\frac{1}{2}} v^*_{i_{max}-\frac{1}{2}} \tag{7.66}$$

After the intermediate velocity is calculated the next step is to calculate the pressure at each segments in one step. This has been done by taking the inverse of the following matrix. Important to notice is that the source/sink term has been implemented in the vector at the right hand side.

$$\frac{1}{\Delta z^2}\begin{pmatrix} -1 & 1 & 0 & 0 & 0 & 0 \\ 1 & -2 & \ddots & 0 & 0 & 0 \\ 0 & \ddots & \ddots & \ddots & 0 & 0 \\ 0 & 0 & \ddots & \ddots & \ddots & 0 \\ 0 & 0 & 0 & \ddots & -2 & 1 \\ 0 & 0 & 0 & 0 & 1 & -2 \end{pmatrix}\begin{pmatrix} p_1^{t+1} \\ \vdots \\ \vdots \\ p_i^{t+1} \\ \vdots \\ p_{i_{max}}^{t+1} \end{pmatrix} = \begin{pmatrix} \frac{A_{mean}}{A_1\Delta t^2}\left(\rho_m^t - \rho_m^{t-1}\right) + \frac{1}{\Delta z\Delta t}\left(\rho^t_{m,in} v^t_{in} - \rho_m v^*_{m,\frac{3}{2}}\right) - \frac{A_3}{A_1\Delta t\Delta z}(\rho_f v^{t+1}_{flow}) \\ \vdots \\ \vdots \\ \frac{A_{mean}}{A_1\Delta t^2}\left(\rho_m^t - \rho_m^{t-1}\right) + \frac{1}{\Delta z\Delta t}\left(\rho_m v^*_{m,i-\frac{1}{2}} - \rho_m v^*_{m,i+\frac{1}{2}}\right) - \frac{A_3}{A_1\Delta z\Delta t}(\rho_f v^{t+1}_{flow}) \\ \vdots \\ \frac{A_{mean}}{A_1\Delta t}\left(\rho_m^t - \rho_m^{t-1}\right) - \frac{\rho_m g i_{max}+\frac{1}{2}}{\Delta z} - \frac{A_3}{A_1\Delta z\Delta t}(\rho_f v^{t+1}_{flow}) \end{pmatrix} \tag{7.67}$$

To determine the flow velocity two methods are proposed. The first one makes the assumption that $p_i^{t+1} = \rho_f g z_i$ i.e. the pressure in the fallpipe is equal to the hydrostatic pressure at that location. The second method determines the flow velocity based on the pressure difference between the in and outside of the fallpipe, following Bernoulli's equation.

7.4.2. FLOW VELOCITY BASED ON LEVELLING OUT PRESSURE DIFFERENCE

The flow velocity can be calculated by making the assumption that the pressure of the new time step is equal to the hydrostatic pressure. This can be done by calculating an intermediate pressure (p^*). This intermediate pressure can be obtained by using equation 7.67 but instead of using the flow velocity of the new time step, the flow velocity is set at 0, resulting in the following equation:

$$\frac{1}{\Delta z^2}\begin{pmatrix} -1 & 1 & 0 & 0 & 0 & 0 \\ 1 & -2 & \ddots & 0 & 0 & 0 \\ 0 & \ddots & \ddots & \ddots & 0 & 0 \\ 0 & 0 & \ddots & \ddots & \ddots & 0 \\ 0 & 0 & 0 & \ddots & -2 & 1 \\ 0 & 0 & 0 & 0 & 1 & -2 \end{pmatrix}\begin{pmatrix} p_1^* \\ \vdots \\ \vdots \\ p_i^* \\ \vdots \\ p_{i_{max}}^* \end{pmatrix} = \begin{pmatrix} \frac{A_{mean}}{A_1\Delta t^2}\left(\rho_m^t - \rho_m^{t-1}\right) + \frac{1}{\Delta z\Delta t}\left(\rho_{m,in}^t v_{in}^t - \rho_m v_{m,\frac{3}{2}}^*\right) \\ \vdots \\ \vdots \\ \frac{A_{mean}}{A_1\Delta t^2}\left(\rho_m^t - \rho_m^{t-1}\right) + \frac{1}{\Delta z\Delta t}\left(\rho_m v_{m,i-\frac{1}{2}}^* - \rho_m v_{m,i+\frac{1}{2}}^*\right) \\ \vdots \\ \frac{A_{mean}}{A_1\Delta t}\left(\rho_m^t - \rho_m^{t-1}\right) - \frac{\rho_m g i_{max}+\frac{1}{2}}{\Delta z}) \end{pmatrix} \tag{7.68}$$

If the intermediate pressure is not equal to the hydrostatic pressure water starts flowing in or out of the element. The pressure difference between the intermediate and hydrostatic pressure can be calculated as follows:

$$\Delta p_i = p_i^* - \rho_w g z_i \tag{7.69}$$

Where p_i^* and z_i are respectively the intermediate pressure and depth at location i. When the pressure difference is calculated and the assumption is made that the pressure in the fallpipe will restore to the hydrostatic pressure, the influence of the source or sink term can be determined by the following equation:

$$\begin{pmatrix} \frac{(A_3\rho_f v_{flow}^{t+1})}{A_1\Delta z\Delta t} \\ \vdots \\ \vdots \\ \frac{(A_3\rho_f v_{flow}^{t+1})}{A_1\Delta z\Delta t} \\ \vdots \\ \frac{(A_3\rho_f v_{flow}^{t+1})}{A_1\Delta z\Delta t} \end{pmatrix} = \frac{1}{\Delta z^2}\begin{pmatrix} -1 & 1 & 0 & 0 & 0 & 0 \\ 1 & -2 & \ddots & 0 & 0 & 0 \\ 0 & \ddots & \ddots & \ddots & 0 & 0 \\ 0 & 0 & \ddots & \ddots & \ddots & 0 \\ 0 & 0 & 0 & \ddots & -2 & 1 \\ 0 & 0 & 0 & 0 & 1 & -2 \end{pmatrix}\begin{pmatrix} \Delta p_1 \\ \vdots \\ \vdots \\ \Delta p_i \\ \vdots \\ \Delta p_{i_{max}} \end{pmatrix} \tag{7.70}$$

Where the vector at the left-hand side is named Q_{flow}. To calculate the in or outflow velocity per element the following equation is used:

$$v_{flow,i} = \frac{Q_{flow,i} A_1 \Delta z \Delta t}{A_3 \rho_f} \tag{7.71}$$

This method can only be applied if the openings between the buckets are large enough, because the flow velocity in or out of the fallpipe for each location is limited by the following equation:

$$v_{flow,i} = \sqrt{\frac{2\Delta p_i}{\rho_f}} \tag{7.72}$$

In the drift-flux model, when the input boundary is fixed a negative pressure can be generated. A negative pressure means that there is no water at that location in the fallpipe i.e. there is a water level drop in the fallpipe. The negative pressure represents the water level drop, an example is given in Appendix A. In reality the relative pressure is equal to 0 Pa when there is no water in the fallpipe. By using equation 7.70, this is not taken into account. Resulting in high flow velocities when the flow area (A_3) goes to zero. When the flow velocity is calculated and the pressure is corrected for the new flow velocities, the mixture velocity for the new time step can be calculated by using equation 7.58.

7.4.3. BERNOULLI'S EQUATION TO DETERMINE FLOW VELOCITIES
The same method as already introduced in paragraph 7.3 can be used as well. Hereby the flow velocity will be calculated by looking at the pressure difference between in and outside of the fallpipe, shown in equation 7.51. This way the flow velocity depends on the pressure difference between in and outside of the fallpipe. Still there can be a negative pressure generated by the model. This should be corrected to 0 Pa i.e. if $p_i < 0$

$p_i = 0$. The pressure difference will be calculated by using the corrected pressure. Important to say is that in this case under-relaxation, small time steps and an iteration loop should be used in the numerical model. A comparison between the two methods is made and discussed in Appendix B.

Comparing the results, it can be said that both techniques can be used to calculate the transport of rocks in the semi-closed fallpipe of Van Oord, because both methods obtain the same results. It can be concluded that for the current dimensions of the buckets and openings between the buckets, the pressure in the fallpipe will restore to the hydrostatic pressure. By making the flow area multiple times smaller, high flow velocities occur by using the assumption that the pressure restores to the hydrostatic pressure, which makes it not a valid method to use. Note that this pressure is a combination of the pressure in the fallpipe and the water added to or subtracted from the fallpipe.

When the flow velocity is calculated, the pressure should be corrected for the new flow velocities to obtain the mixture velocity for the new time step, by using equation 7.58. An overview of the calculation steps is given for the two different methods in Appendix C.

7.4.4. Transport equation for a semi-closed fallpipe
The total velocity of the solids is a combination of the mixture velocity and the settling velocity of the solids, as discussed in chapter 7.2.3. When the total fall velocity per fraction is determined, the transport of concentration for the semi-closed fallpipe can be described.

For a semi-closed fallpipe an overview of the concentration change in an element is displayed in figure 7.15. The concentration change of the element is given by the following equation:

$$\underbrace{\frac{\partial}{\partial t} \int_V \alpha_{s,k} dV}_{\text{Concentration change in time}} + \underbrace{\oint_{A_1} \alpha_{s,k} v_{fall,k} dA_1}_{\text{Concentration inflow}} - \underbrace{\oint_{A_2} \alpha_{s,k} v_{fall,k} dA_2}_{\text{Concentration outflow}} = 0 \qquad (7.73)$$

Important to notice is that area $A_1 = A_2$. The volume of the element is not equal to in or/and outflow area multiplied with Δz, like for a closed fallpipe. This results in the following equation in discrete form:

$$\alpha_{s,k,i}^{t+1} = \alpha_{s,k,i}^t - \frac{A_1 \Delta t}{V} \left(\alpha_{s,k,i-1}^t v_{fall,k,i-1}^{t+1} \right) + \frac{A_2 \Delta t}{V} \left(\alpha_{s,k,i}^t v_{fall,k,i}^{t+1} \right) \qquad (7.74)$$

For solving the transport equation an upwind scheme is used. This means equation 7.74 can only be used to describe the transport of concentration downwards.

The total concentration in each cell can be determined by the summation of the concentration of each fraction in a cell. When the concentration and the velocity in each cell is determined, the production can be calculated. The mixture density should be updated for the following time step by using the following equation.

$$\rho_m^{t+1} = \alpha_s^{t+1} \rho_s + (1 - \alpha_s^{t+1}) \rho_w \qquad (7.75)$$

The new obtained density at each cell is used in the continuity and momentum equation to obtain the pressure term for the new time step. This process continues till the simulation time ends.

7.5. Conclusion
To model the fall process of rock in a fallpipe, the drift-flux model is used. The mixture velocity in the drift-flux model is calculated by using the fractional step method. The fractional step method uses an intermediate velocity and a pressure. To obtain the mixture velocity for the new time step, the intermediate velocity is corrected for the pressure. The total fall velocity is a combination of the mixture velocity in the fallpipe and the settling velocity of the rock, corrected for the hindered settlement and fallpipe influence.

To describe the development of the concentration, the obtained total fall velocity is used in the advection transport equation. In this model the input boundary is fixed, resulting in an under pressure in the fallpipe when the process of rock installation starts. The pressure in the fallpipe will change during the installation process and water will flow in or out of the fallpipe depending on an under or overpressure. The flow velocity in or out of the fallpipe can be calculated by Bernoulli's equation based on the pressure difference in the fallpipe and the hydrostatic pressure or by making the assumption the pressure in the fallpipe will go to the hydrostatic pressure and solve the flow velocity in matrix form.

A big advantage of the matrix method is that the calculation time decreases significantly. Comparing the two methods it can be said that in this case with the given dimensions of the buckets and openings, the

obtained results are equal. The in and outflow of water should be implemented as a mass source and momentum source into respectively the continuity and momentum equation.
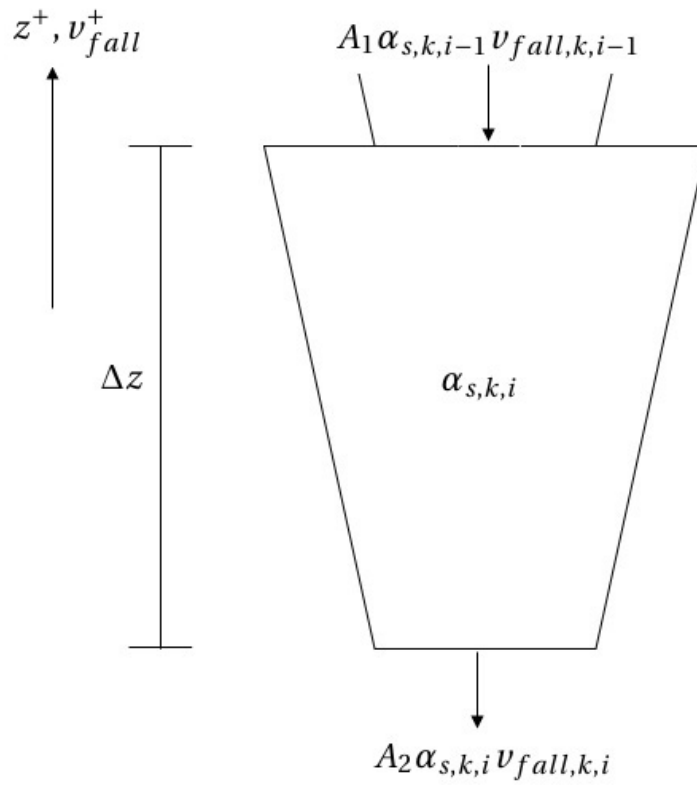

Figure 7.15: Concentration balance over a semi-closed element

8

Model results and Case study

In this chapter an overview of the results is given for the closed and semi-closed fallpipe model. The models will be tested for changing input productions and will be discussed and validated based on measurements provided by Van Oord.

8.1. MODEL PARAMETERS

The standard parameters which are valid for both fallpipe systems are given in table 8.1. Additionally, both fallpipe systems have their own parameters, for example length of segment and pipe diameter. These additional parameters are shown in table 8.2 and 8.3 for respectively the closed fallpipe and semi-closed fallpipe.

Table 8.1: Input parameters used for Matlab model

Symbol	Description	Value	Units
Δt	Time step	0.01	s
L	Length of fallpipe	285	m
g	Gravitational acceleration	9.81	m/s^2
c_d	Drag coefficient	1	–
k	Number of fractions	6	–
d	Diameter of particles	0.022/0.043/0.064/0.085/0.106/0.127	m
λ	Friction factor	0.02	–

Table 8.2: Input parameters for the closed fallpipe system

Symbol	Description	Value	Units
Δz	Length of element	3.0	m
n	Number of elements	95	–
D	Diameter of fallpipe	1.1	m

Table 8.3: Input parameters for the semi-closed fallpipe system

Symbol	Description	Value	Units
L_{bucket}	Length of bucket	2.2	m
θ	Overlap between buckets	0.1	–
Δz	Effective length of element	1.98	m
n	Number of elements	144	–
D_{up}	Upper diameter of bucket	1.1	m
D_{low}	Lower diameter of bucket	0.849	m

8.2. FALLPIPE MODEL FOR WATER FLOW

In this paragraph the results for a water flow in the fallpipe will be discussed. First a water flow without openings in the fallpipe will be described, followed by a fallpipe with openings for water outflow.

8.2.1. CLOSED FALLPIPE FOR WATER FLOW

This model describes the water flow in a fallpipe. Before making the step to a mixture flow, which makes it more difficult, it is good to see how the model is working for a flow with a constant density, i.e. the mixture density is equal to the water density. In table 8.4 an overview is given of the input parameters.

Table 8.4: Input parameters for the water flow model

Input velocity	v_{in}	-2	m/s
Input density	ρ_{in}	1025	kg/m^3

Running the model for 1 second by using the given input values results in the pressure and velocity field, as shown in figure 8.1. What can be seen when looking at the velocity field is that after 1 second the water is flowing in the whole fallpipe. This is because of continuity and the condition that the fluid is incompressible. Important to notice is that in this case the only pressure loss is due to wall friction over the fallpipe.

From the results it can be seen that continuity is conserved. The flow velocity in the fallpipe is equal for all locations, because the density is equal for all locations as well. So, in other words the amount of mass which flows into the fallpipe leaves the fallpipe as well. This is an easy check to see if the model is working as it supposed to do. Furthermore, the overpressure at the top of the fallpipe should be equal to the pressure loss over the fallpipe due to wall friction. The total pressure loss can be calculated in the following manner:

$$\Delta p_{friction} = \frac{1}{2D}\rho_m v_m^2 \lambda_m L \tag{8.1}$$

Substituting the parameters shown in table 8.1 and 8.4, the pressure loss will be 9540 Pa. This number corresponds with the calculated value in the numerical model.
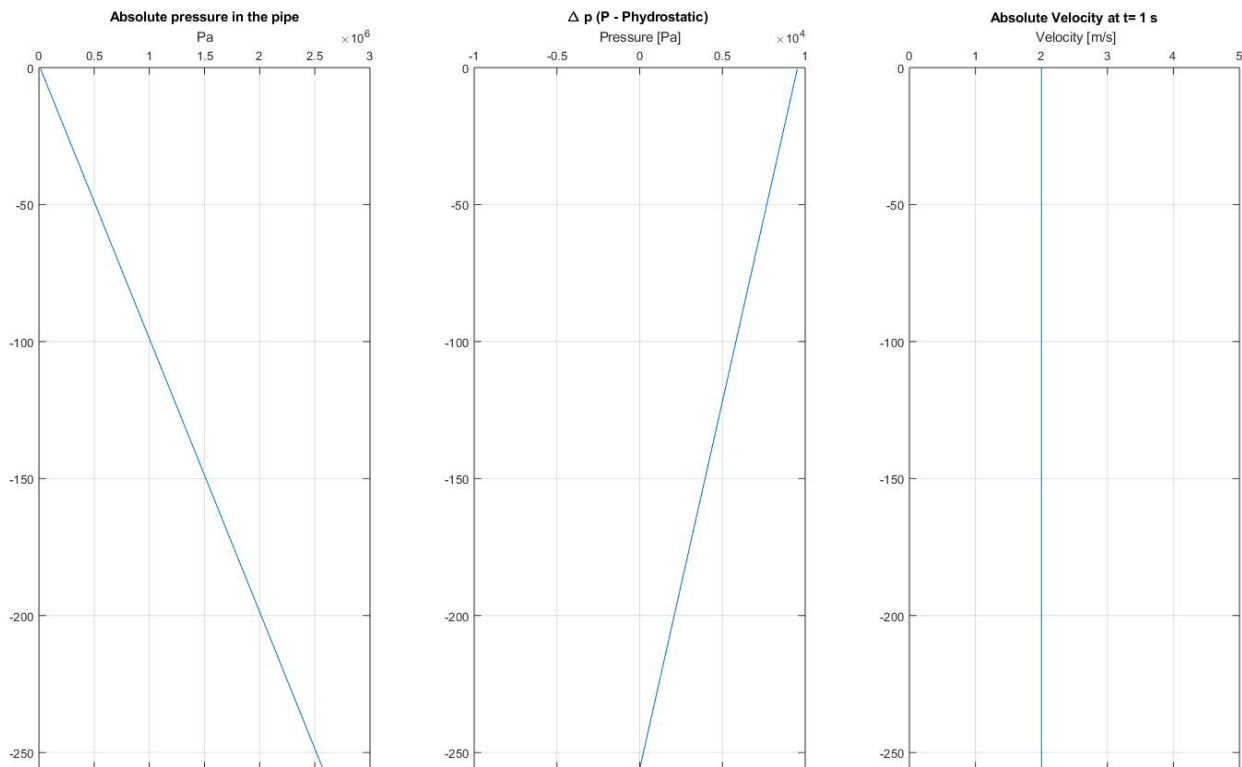
Figure 8.1: Results of water flow in a closed fallpipe

8.2.2. FALLPIPE MODEL FOR WATER FLOW WITH OPENINGS

In this paragraph the results of a water flow in a fallpipe with outlet section will be displayed. The amount of water flowing out depends on the outflow velocity and the outflow area. The overpressure in the fallpipe is a result of the wall friction. A simulation is made with the same input parameters as given in table 8.4. The openings are a fraction of the height of the segment and are chosen as follows: 0, 0.015, 0.025 and 0.05. The location of the outlets are set at: 40, 60, 80, 100 and 120 meter. The results are shown in figure 8.2, 8.3, 8.4 and 8.5. The outflow velocity will be calculated by using the following formula:

$$v_{flow} = \sqrt{\frac{2\Delta p_i}{\rho_f}} \qquad (8.2)$$

It can be clearly seen that by increasing the inflow gap, the pressure inside the fallpipe will go faster to the hydrostatic pressure and the velocity in the fallpipe decreases faster. This is because more water can flow out of the fallpipe due to the larger flow area, resulting in a larger pressure release. When the inflow fraction is equal to zero, the results are equal to the closed fallpipe situation. This is in line with the expectations.
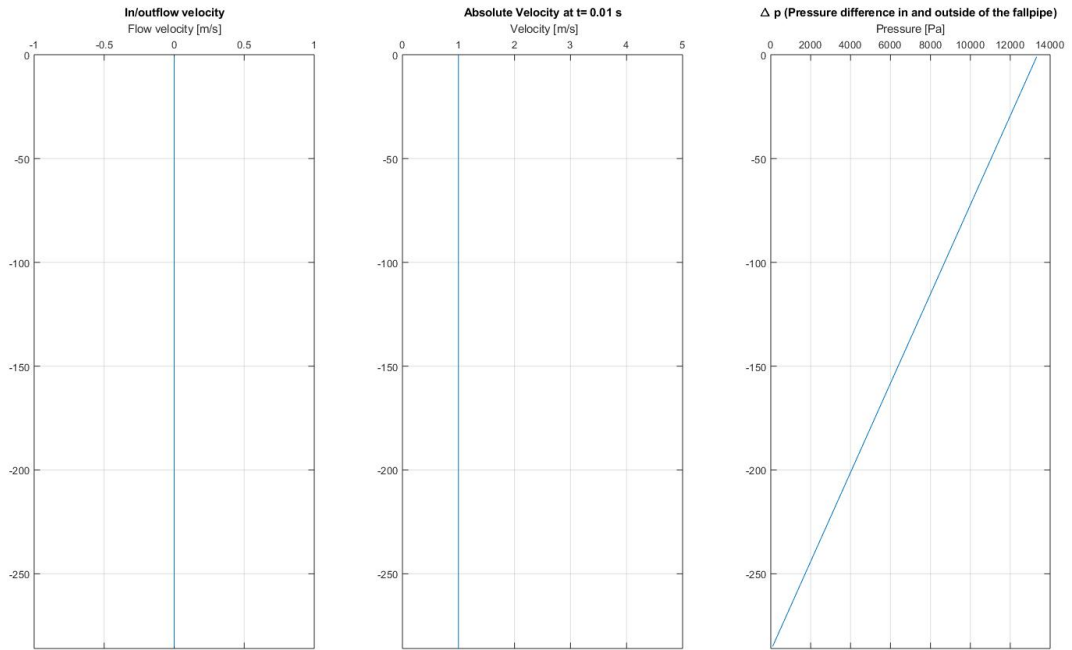
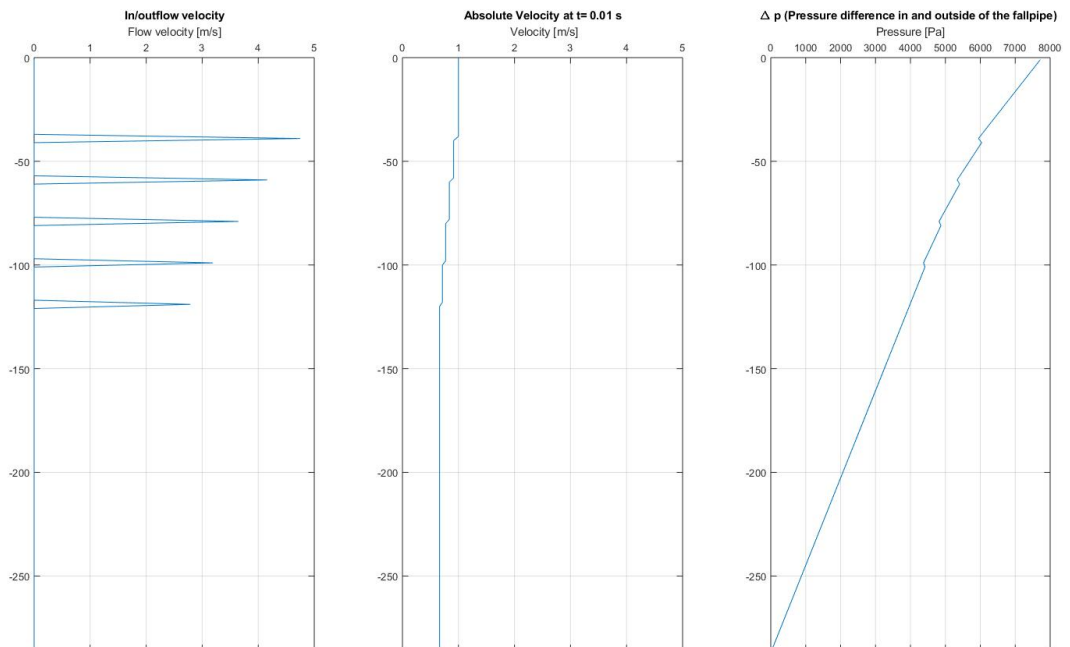Figure 8.2: Results of water flow with outlet fraction 0.0

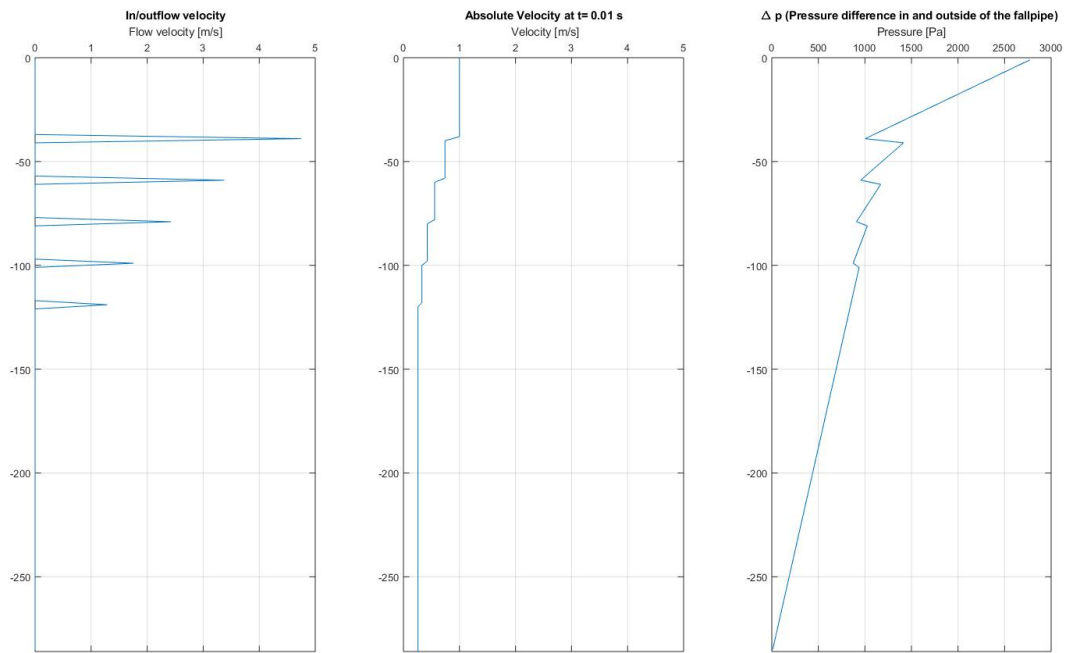Figure 8.3: Results of water flow with outlet fraction 0.015

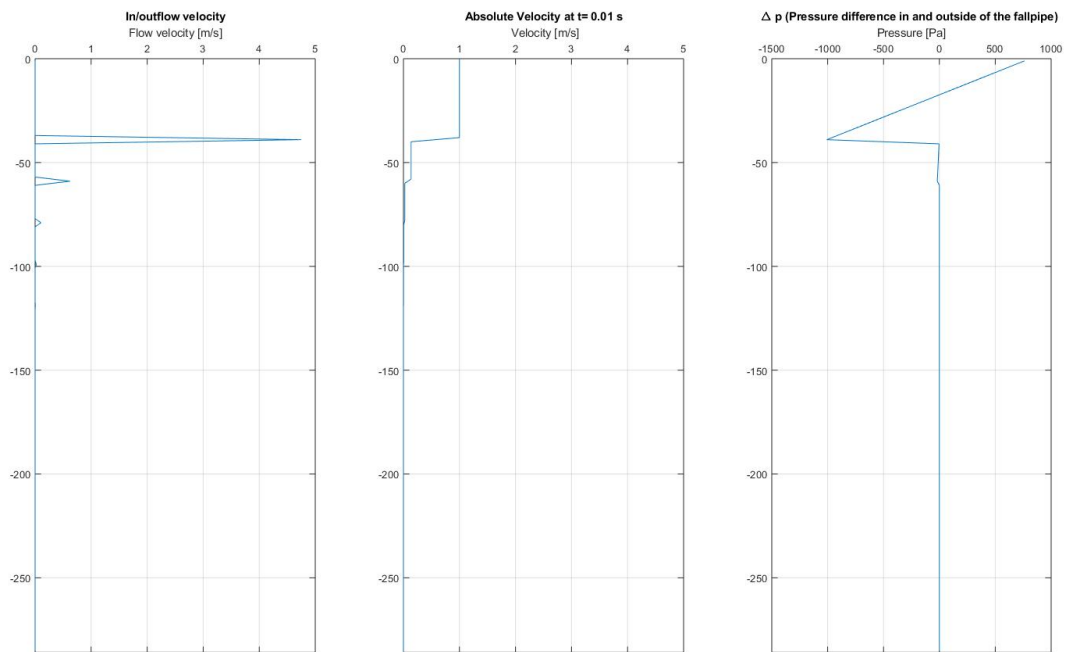Figure 8.4: Results of water flow with outlet fraction 0.025

Figure 8.5: Results of water flow with outlet fraction 0.05

8.3. Closed fallpipe model for rock installation

In this paragraph the results for two different situations are shown. First the results of a closed fallpipe with no water inflow will be discussed, followed by the results of a fallpipe with water in or outflow.

8.3.1. Closed fallpipe with no inlet section

When using a closed fallpipe with no inflow of water, the water level in the fallpipe will drop during the process. This is because of the change of density in the fallpipe resulting in a higher pressure at the end of the fallpipe. To level this pressure difference out, water will flow out at the end of the fallpipe. After some time (depending on water depth and concentration) an equilibrium will be reached.

For the simulation, the production and velocity input is set at 1000 tonnes per hour and 3 m/s respectively. When the input production increases, the input concentration increases as well. In this case the input concentration is calculated at 0.011.

The rocks do not all have the same diameter but may vary in a certain range. In this case it is chosen to divide the rocks in 6 fractions with a particle diameter ranging between 20-125mm, which is commonly used during subsea rock installation. The following results are obtained, shown in figure 8.6.

From the results it can be seen that the model is doing what it is expected to do. The under pressure equals the water level drop and continuity is conserved. The total velocity of the rocks is a combination of the input velocity and the settling of the rock per fraction. The next step is to implement the water flow in or out of the fallpipe if there is an under or over pressure.
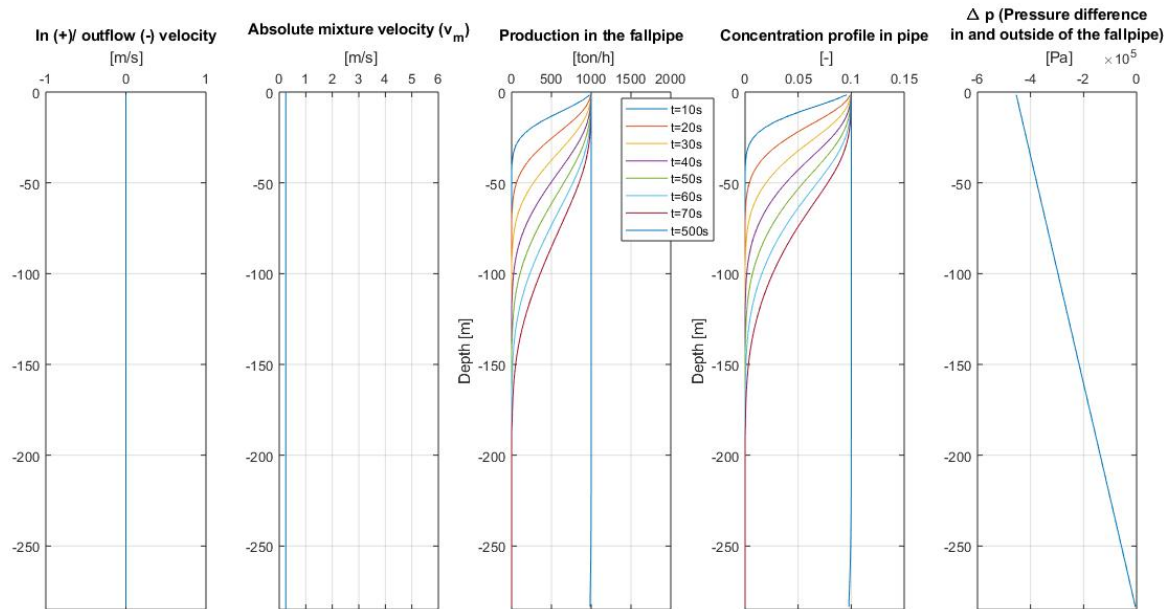

Figure 8.6: Results of a simulation for a closed fallpipe with no openings for different time steps

8.3.2. Closed fallpipe with inlet section

If the water level in the fallpipe drops too far, the pressure difference between the in- and outside of the pipe can be that high that the pipe will implode. To prevent the fallpipe from imploding, there are special inlet segments in a closed fallpipe for allowing water to flow in. To model this it is chosen to implement an inflow area as a fraction of the length of the element at the second element, a couple meters under the water level. If the pressure in the fallpipe is higher than the hydrostatic pressure at the same depth, water will flow out of the element and if the pressure inside the fallpipe is lower, water flows into the element.

A simulation is made by using the same input parameters as in the previous section and an inflow fraction, μ_{area} of 0.25. The inflow fraction is a fraction of the total length of the element (3m). The results are shown in figure 8.7.
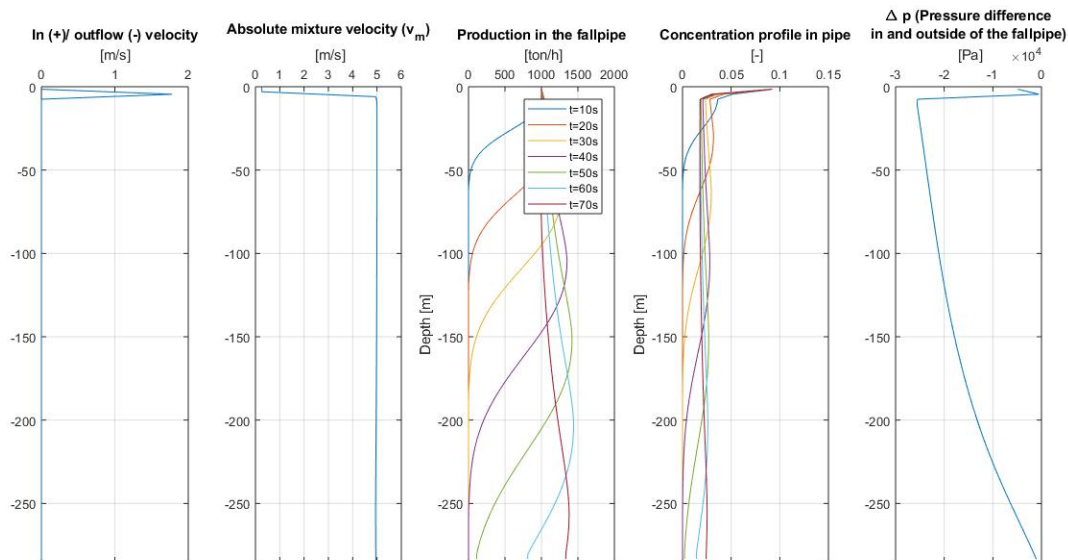
Figure 8.7: Results of simulation of a closed fallpipe with ($\mu_{area} = 0.25$)

Looking at the results it can be clearly seen that the total velocity of the solids in a fallpipe with water inflow is higher than for a closed fallpipe with no water inflow. A higher velocity results in a lower concentration of solids in the fallpipe. Comparing these results with the previous section it can be said that the mixture velocity generated in the fallpipe because of water inflow is a significant contributor to the fall velocity of the solids. The amount of water depends on the inflow velocity and the area of the inflow gap. If the inflow fraction will be set at 0.005 of the length of the element, the following results are obtained. Shown in figure 8.8.
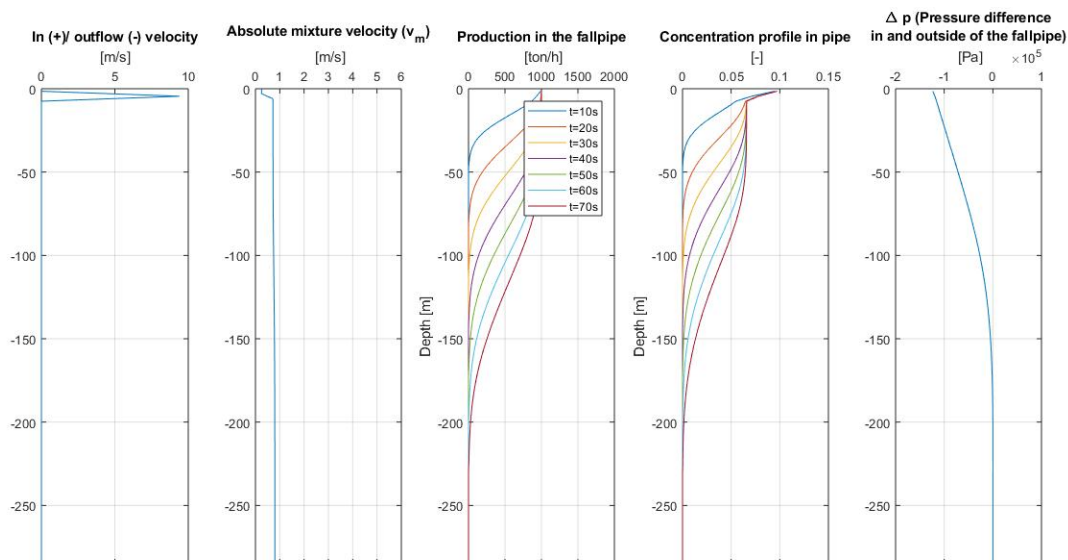
Figure 8.8: Results of simulation of a closed fallpipe with ($\mu_{area} = 0.005$)

Comparing the results of figure 8.7 and 8.8, it can be concluded that the inflow velocity is higher for a smaller inflow fraction. This is in line with the expectations because the amount of water flowing in depends on the inflow velocity and the inflow area. In the second situation it can be seen that the pressure difference between in and outside the fallpipe is not equal to 0 Pa at the location of the inflow. This means that the water

flowing in is not enough to level out the pressure difference. To do this the inflow velocity should be higher than used in this case but this is not possible because the inflow velocity is limited.

The highest inflow velocity which can be obtained is when Δp equals the hydrostatic pressure at that location. If that happens it means there is no water in the fallpipe i.e. relative pressure is 0 Pa. The relative pressure in the fallpipe can not be lower than 0 Pa, resulting in a limited inflow velocity. The maximum inflow velocity at 4.5 m water depth is 9.39 m/s.

It is highly important to check whether continuity is conserved over the element. To check this the second element was looked at. An overview of this segment is given in figure 8.9. The results are shown in table 8.5
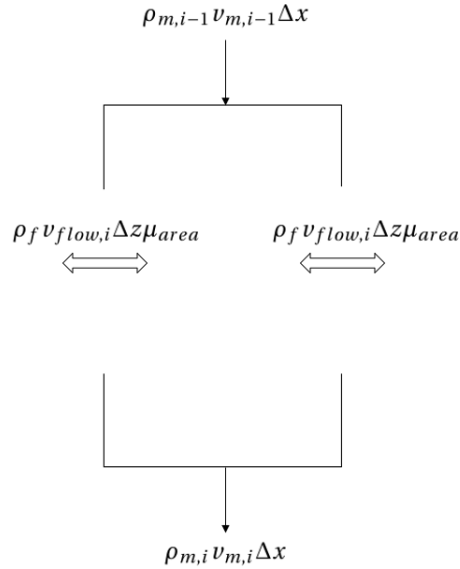
$$\rho_{m,i-1} v_{m,i-1} \Delta x$$

$$\rho_f v_{flow,i} \Delta z \mu_{area} \qquad \rho_f v_{flow,i} \Delta z \mu_{area}$$

$$\rho_{m,i} v_{m,i} \Delta x$$

Figure 8.9: Overview of in and outflow for an open element

Table 8.5: Overview of inflow and outflow of element

Description	Density [kg/m^3]	Absolute velocity [m/s]	Surface [m]
Water inflow	1025	1.68	3
Mixture inflow	1124.5	0.26	1.1
Mixture outflow	1065.7	4.68	1.1

By multiplying the density, velocity and inflow/outflow surface, the mass flow can be calculated. Comparing the mass in and outflow over the element by using the results, shown in table 8.5, it can be seen that the inflow is equal to the outflow and so the continuity is conserved. The total inflow mass is 5493.9 kg/m s and the outflow of mass is 5493.9 kg/m s. So, it can be said that the continuity is conserved.

8.4. SEMI-CLOSED FALLPIPE MODEL FOR ROCK DUMPING

For a semi-closed fallpipe, the Carnot losses should be taken into account, as explained in paragraph 7.4. The Carnot losses are among others depending on the Carnot factor. By using equation **??** and the parameters given in table 8.1, the Carnot factor is calculated at 0.0763. When using three different input productions namely 500, 1000 and 1500 tonnes per hour the following results are obtained see respectively figure 8.10, 8.11 and 8.12. The results are plotted for different time moments.
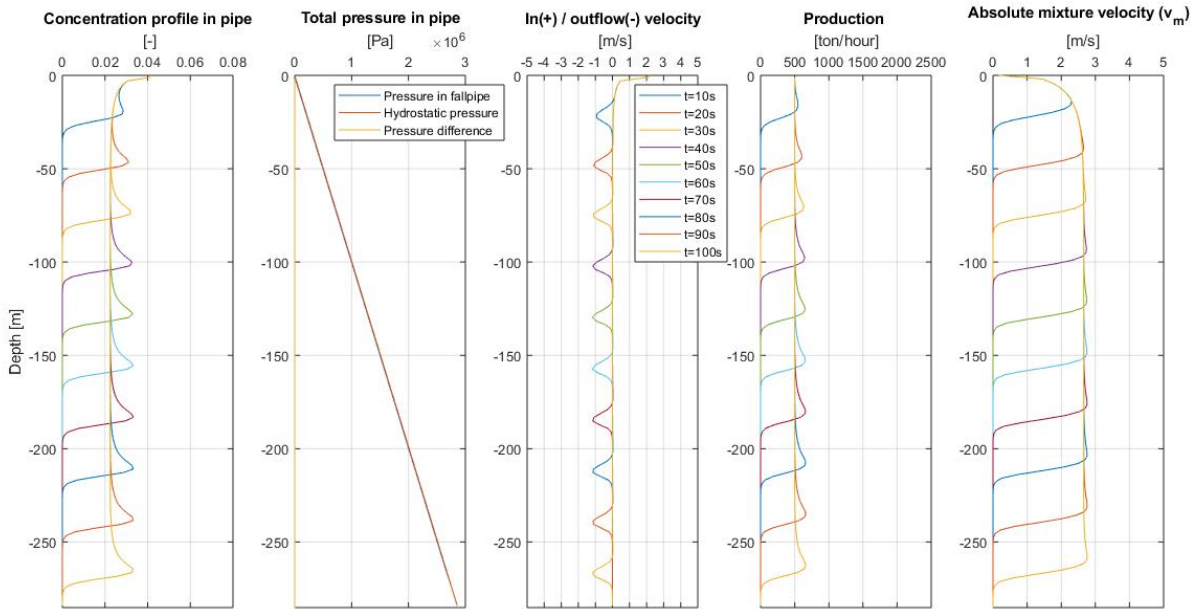

Figure 8.10: Results of the semi-closed fallpipe with input production of 500 ton/h

Comparing the results of the three different input productions, it can be clearly seen that the input production has a large influence on the mixture velocity. When the input production increases the velocity increases as well. This is because a higher production means a higher mixture density in the fallpipe, resulting in a higher pressure difference at the end of the fallpipe and a larger water level drop. A larger water level drop results in more water flowing in, when the inflow area stays constants the flow velocity will increase. This results in a higher velocity in the fallpipe by increasing the production. When looking at the in and outflow velocities between the gaps of the buckets it can be seen that by increasing the production the outflow velocity will increase as well.

The bulk velocity will go to zero when the concentration goes to zero because the pressure at the front will decrease linear with the concentration. When the pressure is hydrostatic and there is no concentration in the element, the mixture velocity will be zero. This is displayed in figure 8.10, 8.11 and 8.12.
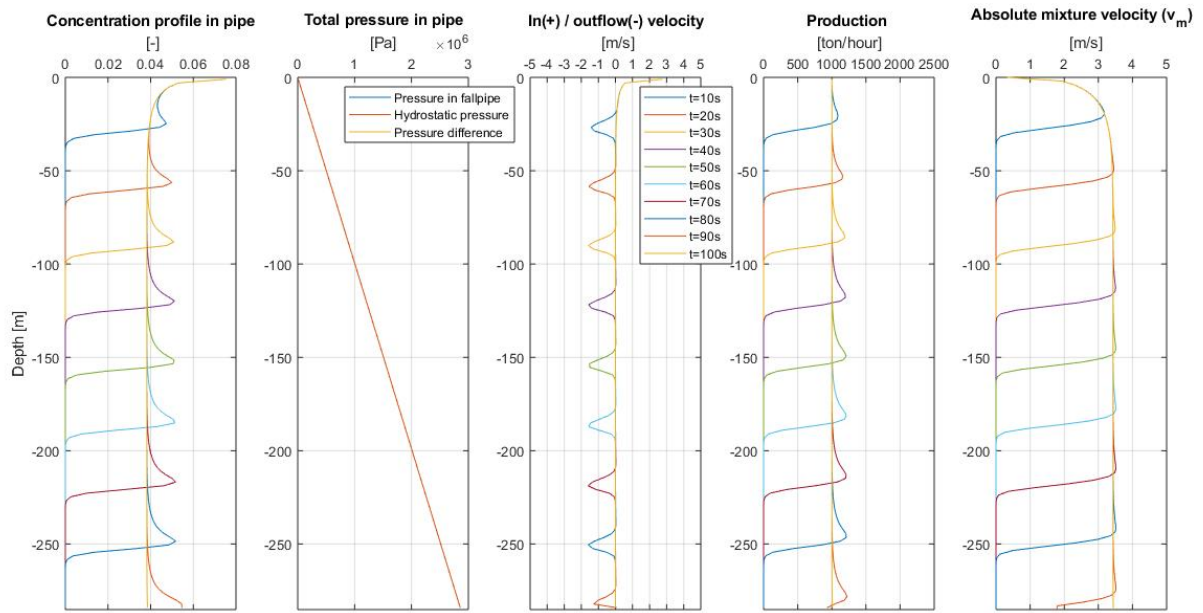
Figure 8.11: Results of the semi-closed fallpipe with input production of 1000 ton/h
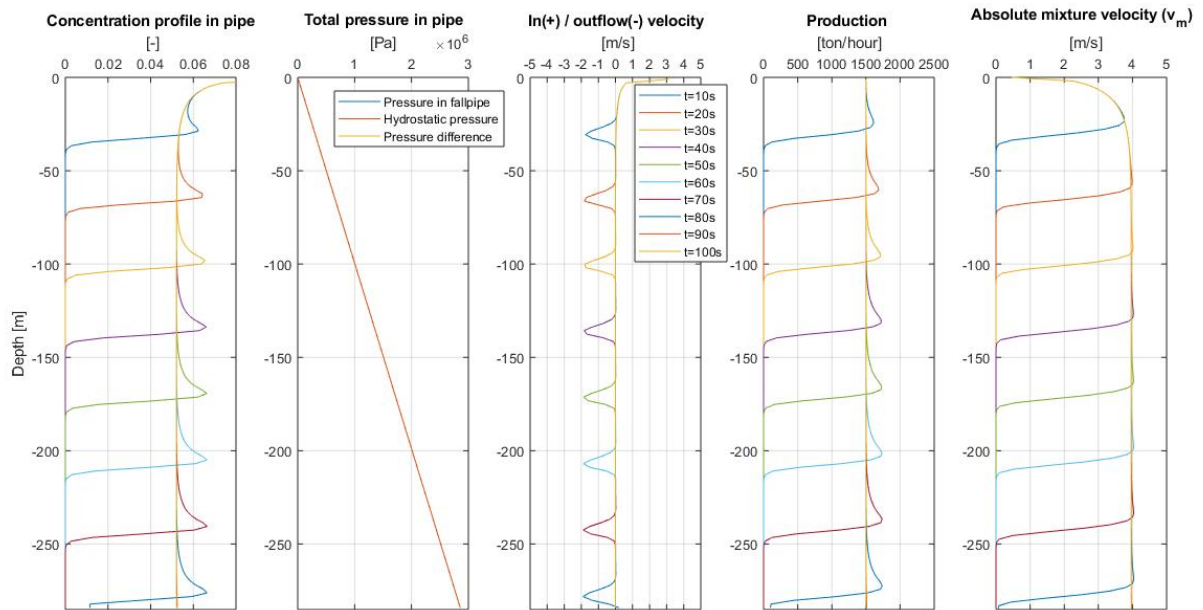

Figure 8.12: Results of the semi-closed fallpipe with input production of 1500 ton/h

8.5. CONCLUSION

In this chapter the results are shown for a fallpipe with water flow, a fallpipe with water flow and openings, a fallpipe with rocks and an inlet section and a semi-closed fallpipe with openings at each element. The influence of the water in and outflow can be clearly seen. The mixture velocity in the fallpipe increases significantly with the possibility of water inflow. When comparing the semi-closed fallpipe model with the measurements provided by Van Oord, it can be said that the model provides a good prediction of when the front of the rocks are leaving the fallpipe. The falling time is exactly the time between input production at the top of the fallpipe and output production at the end of the fallpipe. The concentration changes can be quite accurately predicted, meaning that the falling time is accurate as well. The absolute value of the concentration is more difficult to validate because the measurements are not giving an answer to that due to the fluctuations of the measurements.

9

Final conclusions and recommendations

During this thesis, research has been carried out into the fall process of rock in a fallpipe. The main objective was to provide a better understanding of the production, concentration and velocity profile in the fallpipe during subsea rock installation. In this chapter the general conclusions and recommendations for further research will be discussed.

9.1. CONCLUSIONS

- The fall process of rock during subsea rock installation can be modelled in one dimension by using the drift-flux model. The drift-flux model uses a general mixture velocity and a slip velocity. The mixture velocity can be calculated by the fractional step method and the slip velocity can be calculated by the hindered settling theory. Combining these two velocities results in the total fall velocity of a rock particle. To describe the concentration in the fallpipe, the total fall velocity of the rock is used in the transport equation.

- An important difference between rock falling in a closed fallpipe and a semi-closed fallpipe is that for a semi-closed fallpipe an extra pressure loss should be implemented in the momentum equation: The Carnot loss.

- By using a closed fallpipe during subsea rock installation, the inflow area can be adjusted, while for a semi-closed fallpipe the inflow area is fixed. This means the amount of water flowing into the fallpipe can be controlled for a closed fallpipe, while this is not the case for a semi-closed fallpipe. When the amount of water can be adjusted, the flow velocity and so the total fall velocity of the rocks can be controlled.

- When rocks are starting to fall into the fallpipe the density in the fallpipe increases. When the density increases, the pressure in the fallpipe increases as well. To level this out, the water level in the fallpipe will drop. If the water level drops too far, water from outside the fallpipe will start flowing in. This process continues till the production stops and the density in the fallpipe restores to the density of water.

- The inflow of water from outside the fallpipe into the fallpipe can be modelled as a mass source in the continuity equation and as a momentum source into the momentum equation.

- The assumption that the in and outflow of water results in a pressure in the fallpipe, which is equal to the hydrostatic pressure, has been checked by calculating the in and outflow based on the pressure difference between in an outside the fallpipe. The results of both calculations are the same, which means by the given parameters of the buckets and inflow gap the pressure will restore to the hydrostatic pressure in the fallpipe.

- The model can be used to give a good prediction of the total falling time with varying input production. The results of the model are checked by performing a case study with input production and concentration measurements and the concentration changes can be clearly seen and match with the model

results. The measurements of the case study cannot be used to determine the absolute value of the concentration in the fallpipe because the measurements are not consistent. Important to say is that the inflow area is large enough to ensure the inflow velocity will not exceed the maximum inflow velocity.

- For a semi-closed fallpipe the outflow velocities between the buckets are in the range of 1-2 m/s for productions between 500-1500 tonnes per hour. Comparing these velocities with the settling velocity of small diameter rocks, a tentative conclusion can be made that in some circumstances small rocks can flow out of the fallpipe through the opening between the buckets.

9.2. RECOMMENDATIONS

- The concentration changes can be clearly seen in the measurements but the absolute value of the concentration is varying too much to use as a correct result and to validate the model. To give more value to the model, velocity measurements should be carried out to determine the output velocity of the rock at the end of the fallpipe. By combining the velocity and concentration measurements, the model can be tested more precisely.

- When using a semi-closed fallpipe, a question that arises is: "Can rocks flow out of the fallpipe through the openings between the buckets?" A tentative conclusion can be given while looking at the settling velocity of small diameter rocks and the outflow velocities between the buckets. Based on this observation it can be said that there is a chance that rocks flow out of the fallpipe through the openings between the buckets. To give a more precise answer on which diameter rocks will flow out, a test set up could be made, to simulate the fall process and determine at which outflow velocities rocks will start flowing out.

- The model is only tested for water depths up to 300 meters because no measurements are carried out for larger depths. This range is a quite regular working depth for subsea rock installation. To validate and determine the accuracy of the model in deeper waters, measurements in larger water depths should be carried out.

Bibliography

de Jong, Rob. 2002. *Calculation of equilibrium flow velocity in semi-closed fallpipe without using chain calculations.* Tech. rept. Technical report, van Oord E&E Dredging Research, Rotterdam.

Es, A Van. 2009. *Fallpipe model FFPV Nordnes.* Technical report, van Oord E&E dredging research.

Ferguson, R.I., & Church, M. 2004. A Simple Universal Equation for Grain Settling Velocity. *Journal of Sedimentary Research,* **74**(6), 933.

Goeree, J.C., & van Rhee, C. 2013. *Numerical Sediment Simulation using a Continuous Flow Model.* Tech. rept. January. Delft University of Technology.

Goeree, J.C., Keetels, G.H., Munts, E.A., Bugdayci, H.H., & van Rhee, C. 2016. Concentration and velocity profiles of sediment-water mixtures using the drift flux model. *The Canadian journal of chemical engineering,* **94**(6).

Hirsch Charles. 2007. *Numerical computation of internal & external flows.* 2 edn. Burlington,USA: Butterworth_Heinermann.

Jop, P, Forterre, Y, & Pouliquen, O. 2006. A constitutive law for dense granular flows. *nature,* **441**, 727–730.

Kevelam, M. 2016. *Hydrodynamics below a fallpipe, The profile of a rock berm acquired with rock placement operations.* Master's thesis, Delft University of Technology.

Li, Mingzhong, Zhang, Guodong, Xue, Jianquan, Li, Yanchao, & Tang, Shukai. 2014. Prediction of the wall factor of arbitrary particle settling through various fluid media in a cylindrical tube using artificial intelligence. *The Scientific World Journal,* **2014**.

Matoušek, V. 2004. *Dredge pumps and slurry transport.* Lecture notes, Delft University of Technology.

Miedema, S.A. 1981. *The flow of dredged slurry in and out hoppers and the settlement process in hoppers.* Master's thesis, Delft University of Technology.

Ravelli, F.D.C. 2012. *Improving the efficiency of a flexible fallpipe vessel: An experimental study on the spreading of rock in an impinging plane jet.* Master's thesis, Delft University of Technology.

Reus, J S De. 2004. *Het valgedrag van stortsteen onder invloed van stroming.* Master's thesis, Delft University of Technology.

Richardson, J.F., & Zaki, W.N. 1997. Sedimentation and fluidisation: Part I. *Chemical Engineering Research and Design,* **75**(3), S82–S100.

Rook, Dirk. 1994. *Fall pipe fluid mechanics.* Master's thesis, Delft University of Technology.

Rowe, P.N. 1987. A convenient empirical equation for estimation of the Richardson-Zaki exponent. *Chemical engineering research,* **42**(2795-2796).

Van Rhee, C. 2017. *Dredging process II.* Lecture notes, Delft University of Technology, Delft.

Wijk, J M Van. 2011. *Vertical Hydraulic Transport for deep sea mining, A study into flow assurance.* PhD thesis, Delft University of Technology.

On the fall process of rock during Subsea Rock Installation

Master thesis

Part III

Appendices

A

Calculations of water level drop

During the fall process of rock in the fallpipe, an under pressure is generated by the drift flux model. In this Appendix, it is shown that the under pressure generated by the model equals the water level drop in the fallpipe. To do this a comparison is made between the under pressure in the fallpipe and the hydrostatic pressure of the column. In this simulation the fallpipe is only open at the top end and the lower end of the fallpipe. Important to notice is that there will be no water added or subtracted when there is an under or overpressure.

Under pressure in fallpipe
In this case the duration of the simulation is set at 800 seconds, to ensure an equilibrium situation is reached. The input production is set at 700 tonnes per hour which results in an input mixture density of 98.13 kg/m^3. The total length of the fallpipe is 301 m. While running this model the following results are obtained, see figure A.1.
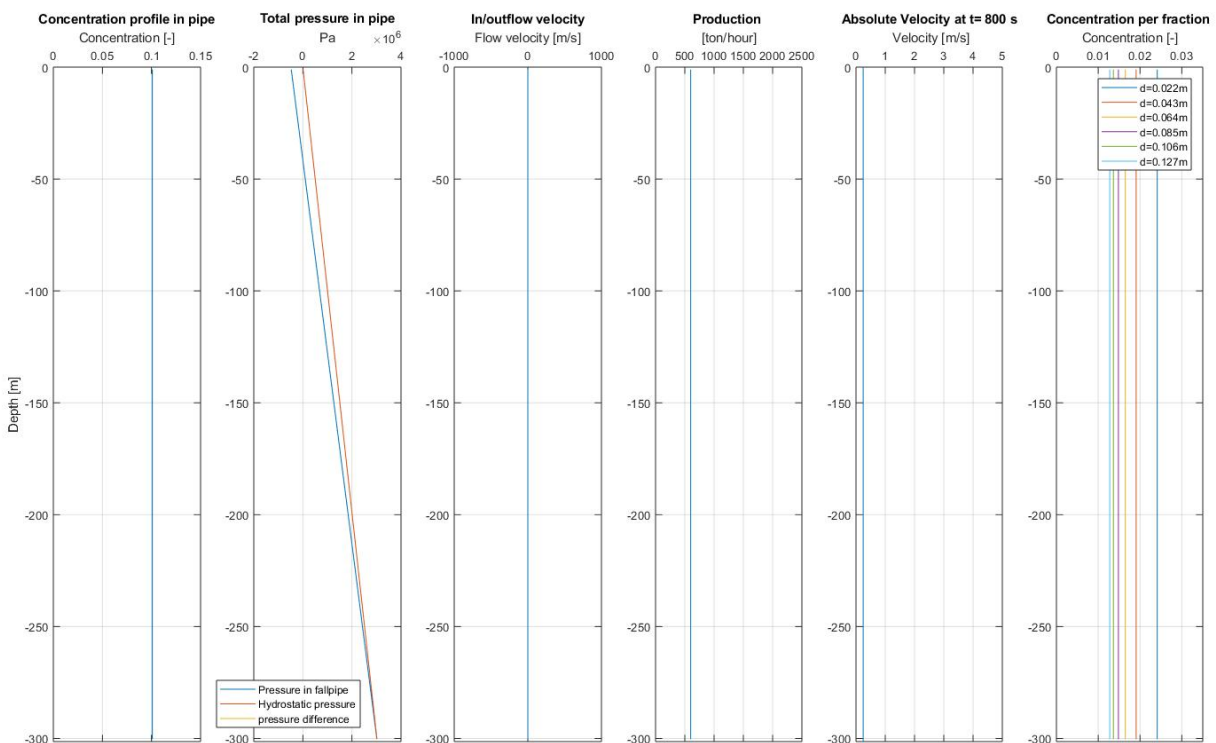

Figure A.1: Results for water level drop calculations

67

The under pressure at location 1, as shown in figure A.2 can be calculated and is $4.98 \cdot 10^5$ Pa. This pressure should be equal to the pressure generated by the mixture density in the fallpipe multiplied with the gravitational constant multiplied with the height of the water level drop.
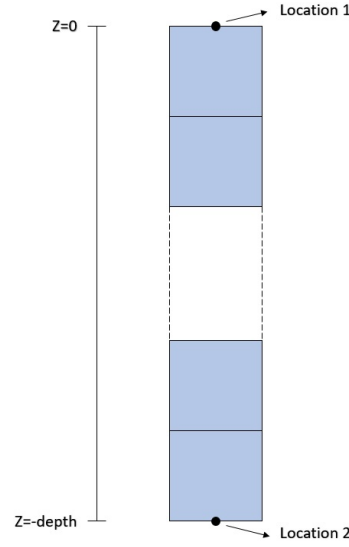

Figure A.2: Location of the under pressure used for calculation

To calculate the water level drop based on the under pressure the following equation can be used.

$$z_{drop} = \frac{p_1}{\rho_m g} \tag{A.1}$$

Where p_1 is the pressure at location 1. and the mixture density in the fallpipe in this case is equal to 1188.9 kg/m^3. Filling in the given parameters results in a z_{drop} of 41.54 m.

Static pressure water
When the fallpipe is completely filled with water. The static pressure at the end of the fallpipe can be calculated by using the following equation.

$$p = \rho_f g L \tag{A.2}$$

Where L is the length of the fallpipe. Filling in the parameters results in a hydrostatic pressure of the water column at location 2 (see figure A.2) of $3.03 \cdot 10^6$ Pa.

Static pressure mixture density
The static pressure at location 2 by using the mixture density should be equal to the static pressure by using the density of water. While looking at equation A.2 and saying the mixture density is higher than the water density, the height of the mixture column (z) should be smaller than the height of water column i.e. equation A.3 should be valid.

$$\rho_f g L = \rho_m g z \tag{A.3}$$

To calculate the height of the column for the mixture case, equation A.3 can be rewritten to the following equation.

$$z = \frac{\rho_f g L}{\rho_m g} \tag{A.4}$$

Filling in the given parameters results in a column height (z) of 253.48 m. The water level drop is therefore 301-259.86 = 41.57 m.

Conclusion

The water level drop based on the theory of Bernoulli is 41.54 m. While the model calculates a water level drop of 41.57 m. This difference can be written to the location of the pressure. In the model the pressure is located in the middle of the element. While the calculation is using the pressure at the boundary. For the model the pressure at the boundary is estimated.

B

Comparing the two calculation methods for flow velocities

In this Appendix, a comparison is made between the two calculation methods for the outflow velocity. The first method is based on the assumption that the pressure in the fallpipe goes to the hydrostatic pressure and the second method is using Bernoulli's equation to calculate the flow velocity between the buckets.

By implementing the flow velocity based on Bernoulli's equation, under-relaxation and an iteration scheme should be used. A big advantage of the first method is that the calculation time is significant lower than for the second method but it assumes that the pressure in the fallpipe is always equal to the hydrostatic pressure. Which can only be true if the flow area (opening between the buckets) is large enough so the flow velocity will not exceed the maximum flow velocity.

Firstly, a comparison is made between the two models after a simulatin of10 seconds. The results are plotted in one figure and shown in figure B.1. The length of the fallpipe is set at 100m and the input production is 1000 tonnes per hour.
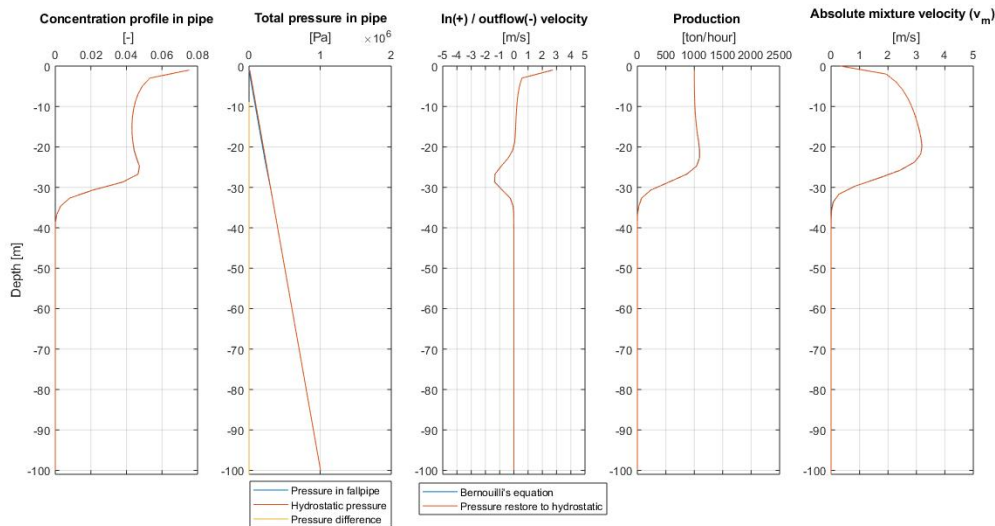

Figure B.1: Results of simulation comparing the two methods for flow velocity at t=10s

When looking at the results, it can be seen that both methods calculates exactly the same results, because both lines are on top of each other. Meaning that the pressure in the fallpipe for the given dimensions of the buckets and openings will restore to the hydrostatic pressure. It is of interest to see what happens with the flow velocity and the mixture velocity if the flow area increases or decreases.

71

Increase of flow area

First the flow area is made two times larger. The flow velocity should therefore be two times smaller, as can be seen in figure B.2. Still it can be seen that the pressure in the fallpipe restores to hydrostatic pressure.
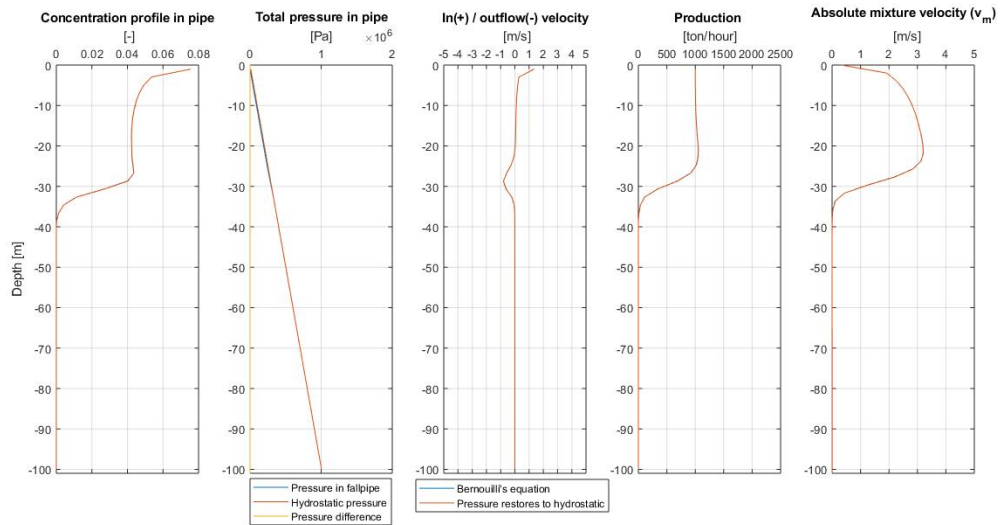

Figure B.2: Results of simulation comparing the two methods for flow velocity at t=20s with flow area 2 times larger than original

Decrease of flow area

Looking at the first method, when decreasing the flow area to zero, the flow velocity should go to infinity. Following Bernoulli, the flow velocity is limited by the pressure difference between in and outside the fallpipe this can not be the case in reality. The method based on Bernoulli's equation for calculating the flow velocities takes into account that the flow velocity will not exceed the maximum flow velocity based on the pressure difference in and outside of the fallpipe. A comparison is made in figure B.3 by using a flow area which is 10 times smaller than the original area. The simulation time is in this case 20 seconds.
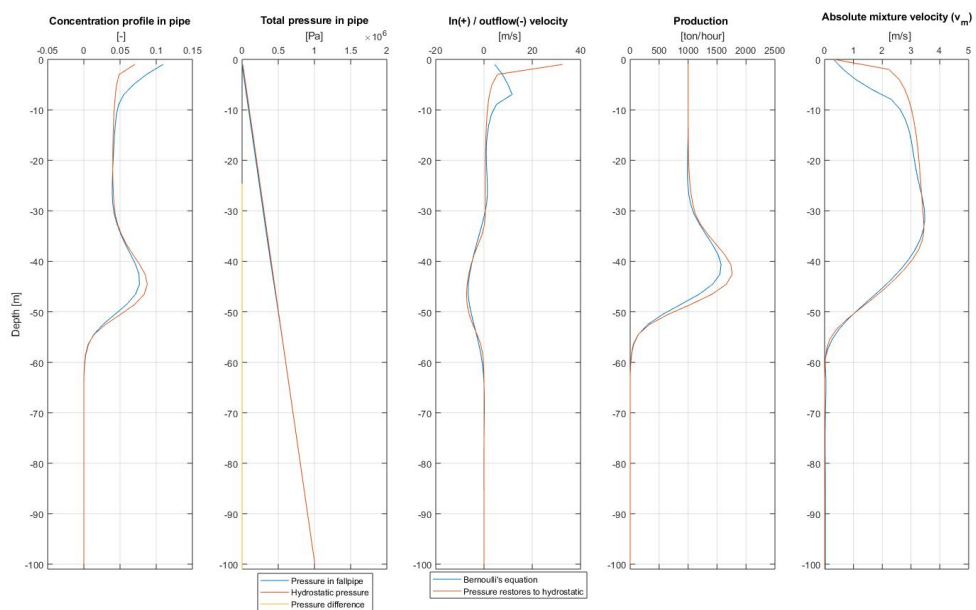

Figure B.3: Results of simulation comparing the two methods for flow velocity at t=20s with flow area 10 times smaller than original

In figure B.3, it can already be seen that the two methods obtain different results. First, the mixture velocity needs more time to develop by taking into account the limited flow velocity. Second, because of the difference

in mixture velocity, the concentration profile looks different as well and finally the inflow velocities at the top of the fallpipe are different. By making the flow area 100 times smaller than original, the results displayed in figure B.4 are obtained. It can be clearly seen that the flow area has a significant influence on the mixture velocity.
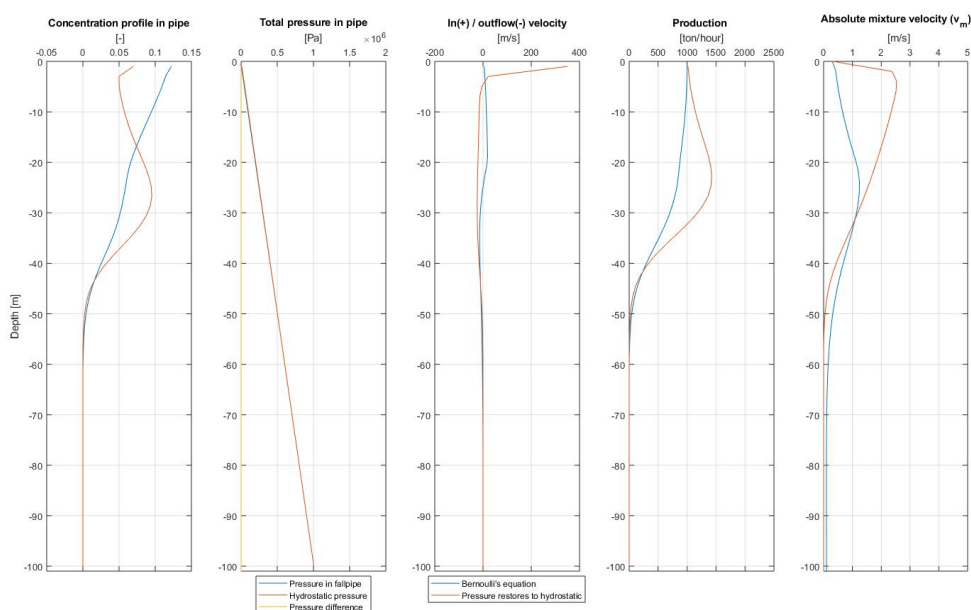

Figure B.4: Results of simulation comparing the two methods for flow velocity at t=20s with flow area 100 times smaller than original

While running both methods till an equilibrium is reached (the fallpipe is filled with concentration) the results, shown in figure B.5 are obtained. Again, it can be clearly seen that the area has a significant influence on the development of the mixture velocity. When the mixture velocity changes the transport of concentration changes as well.
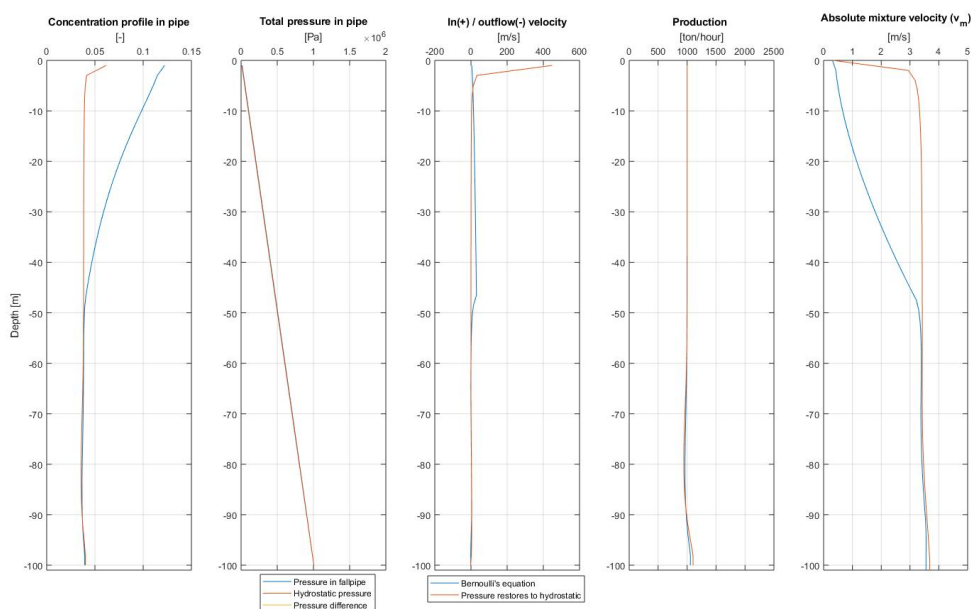

Figure B.5: Results of simulation comparing the two methods for flow velocity till an equilibrium is reached with a flow area 100x smaller than original

Finally, it can be said that by using the current dimensions of the semi-closed fallpipe system of Van Oord both methods will provide the same outcome. By increasing the flow area still both methods provide the same results. An increase in the flow area results in a decrease of the flow velocity. When the openings between the buckets decreases, the two methods will not give the same results any more. The first method does not take into account the limited flow velocity, while the second method does take it into account. This will result in different outcomes by decreasing of the flow area.

C

Schematic overview of calculations steps

In this Appendix an overview is given of the calculation steps of the two methods used for calculating the in and outflow velocities. In figure C.1, the matrix method is displayed and in figure C.2 an overview of the iteration method is shown.
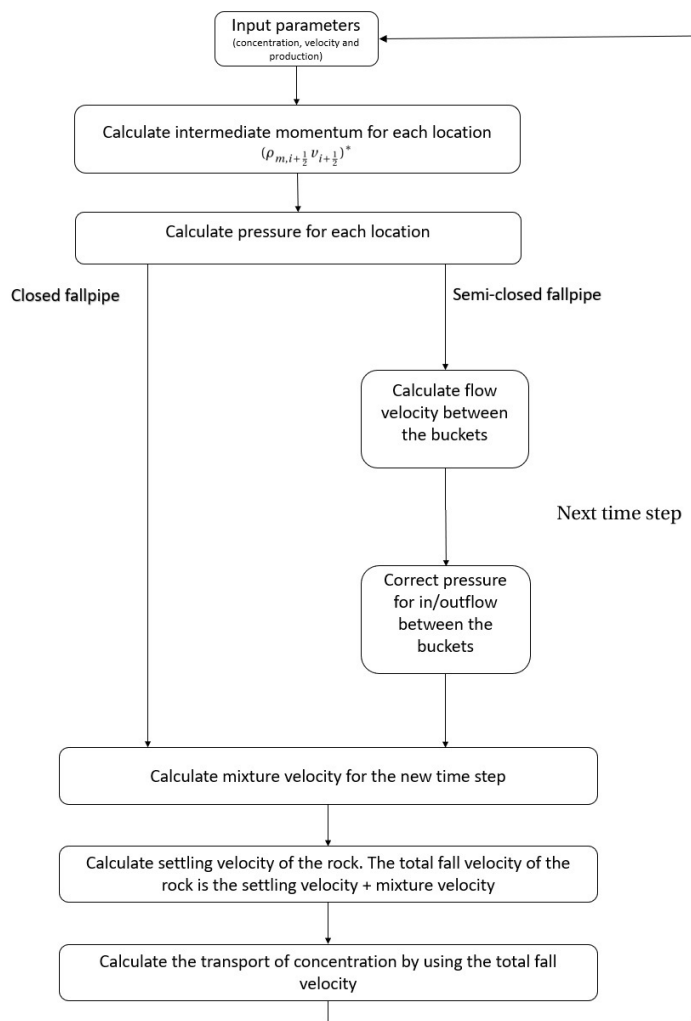

Figure C.1: Schematic overview of calculation steps for closed and semi-closed fallpipe
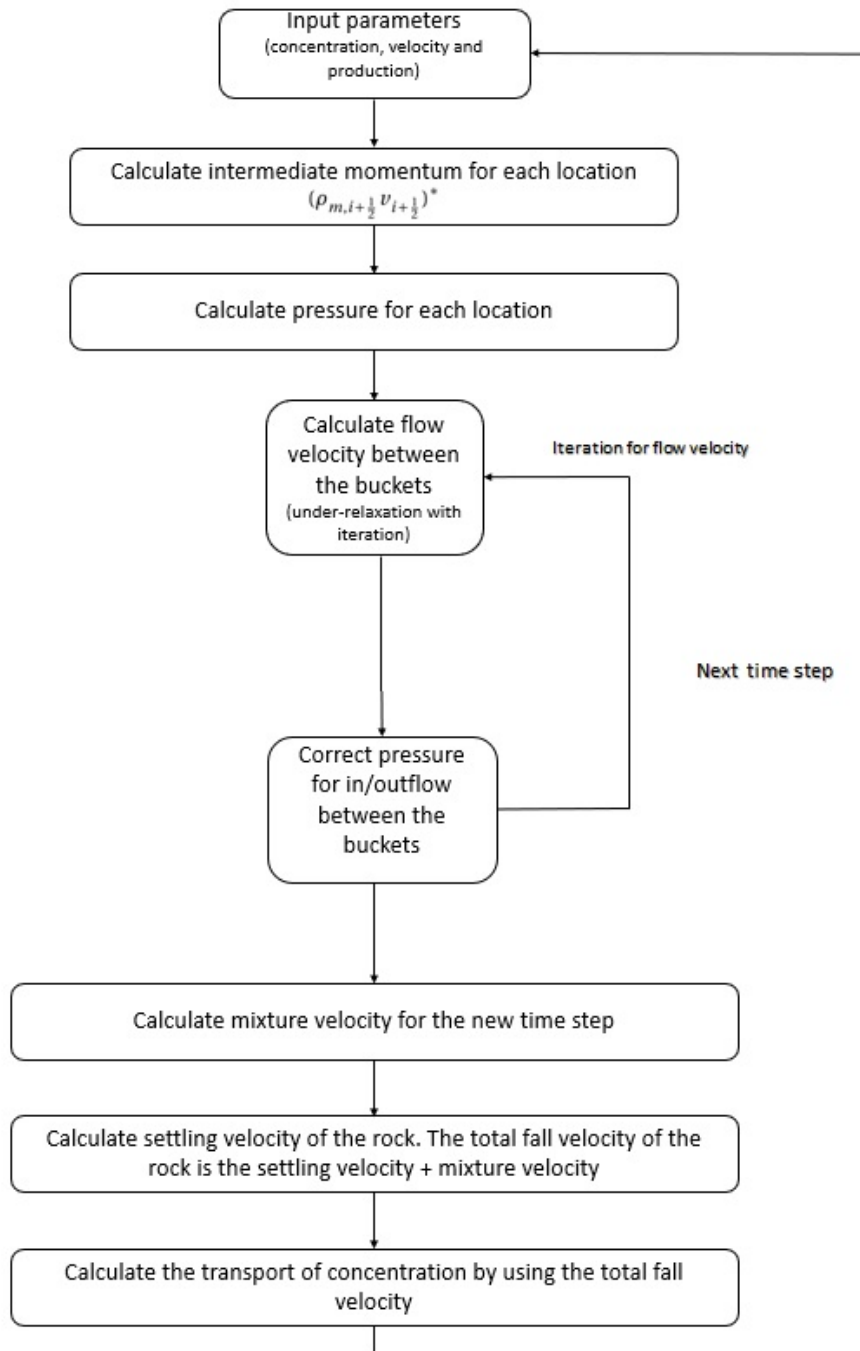
Figure C.2: Schematic overview of calculation steps with iteration for a semi-closed fallpipe